The impact of shading systems on indoor comfort and energy-efficiency for offices: Comparative analysis of **fabric roller blinds** and **electrochromic glazing** under automated and manual controls

Politecnico di Torino
École Polytechnique Fédérale de Lausanne

Master's Degree in Architecture for Sustainability

Politecnico di Torino

EPFL

The impact of shading systems on indoor comfort and energy-efficiency for offices: Comparative analysis of fabric roller blinds and electrochromic glazing under automated and manual controls

Supervisors
Prof. Valerio Lo Verso
Dr. Jan Wienold

Candidate
Mojdeh Sabeti

21 August 2025

Abstract

High-performance façades are expected to reduce operational energy while safeguarding occupants' comfort, yet comparing dynamic shading technologies under realistic control was not widely discussed in previous research. This thesis therefore benchmarks comparison of electrochromic (EC) glazing against fabric roller blinds—mounted either inside or outside—when both are driven by similar sensor-based algorithm with manual override (simulation-based). A south-facing, two-desk office was modelled for three representative European climates—Northern European (Stockholm), Central European (Frankfurt), and Southern European (Rome). Annual heating, cooling, and interior lighting loads, spatial daylight autonomy (sDA), 95th-percentile Daylight Glare Probability (DGP), and melanopic daylight autonomy (mel-DA, the percentage of daytime hours which melanopic EDI $\geq$ 250 lux) were computed and compared.

Overall, the differences between the various configurations in terms of overall performance are small. All seven façade variants occupied a narrow energy band: the sum of heating, cooling, and lighting never differed by more than $10\,\mathrm{kWh\,m^{-2}\,yr^{-1}}$. Lighting loads remained modest: the worst fabric raised annual lighting by only $\approx 1\,\mathrm{kWh\,m^{-2}\,yr^{-1}}$ versus the best.

Daylight-related metrics showed similarly subtle spreads. Exterior blinds boosted sDA by 4–11% in Stockholm and Frankfurt but reduced it in Rome; EC glazing stayed within the top performer in every city regarding daylight provision. All fabric options kept DGP in the "imperceptible glare" EN-17037 band, whereas EC raised that value by 0.01—just enough to shift the rating to "perceptible glare". Mel-DA exceeded 70% for every configuration in the two cooler climates and ranged from 65% to 88% in Rome, where exterior and light-coloured fabrics excelled.

A sensitivity analysis of activation thresholds and signals revealed that revising the glare-avoidance and solar-gain triggers influenced the shading performance significantly, in terms of both energy demand and occupant comfort. The study therefore concludes that, within today's high-performance envelope, an optimised, occupant-centred control strategy is more decisive than the choice between the shading technologies. Architects and practitioners are advised to prioritise calibrating control logic based on local climate and perceptual metrics to create buildings which are sustainable, energy-efficient, and occupant-friendly.

Thesis-Derived Publications

- **Sabeti, M.**, Khodaei Tehrani, H., Lo Verso, V.R.M. and Wienold, J. (2025) "Comparing the performance of electrochromic glazing and fabric blinds under manual and automated control schemes". *CISBAT Conference*, Lausanne, Switzerland, September 2025. Forthcoming online November 2025.

  Abstract. This study compares the performance of electrochromic (EC) glazing and fabric roller blinds under automated control with manual override in office buildings across three European climates including Stockholm, Frankfurt, and Rome. A simulation-driven methodology using a single-office layout with dual occupancy assessed key performance metrics: energy demand, indoor daylight provision, daylight glare, and daylight-induced non-visual potential. Fabric blinds were evaluated in both internal and external configurations, paired with solar control or Low-E glazing. EC glazing was analysed with independently controlled upper and lower window sections. Realistic sensor-triggered control strategies with specified thresholds were applied. Results show overall differences between shading solutions are modest. However, external shading and EC enhance energy efficiency in cooler climates (Stockholm and Frankfurt), while in Rome, EC glazing performs similarly to internal shading. EC also exhibits a slight increase in glare for all investigated climates. Spatial daylight autonomy was the highest for external shading in cooler climates and lowest in Rome, and non-visual potential were high for all systems in Stockholm and Frankfurt, while it shows variations in Rome. This study also concludes that control strategy plays a more decisive role in optimizing façade performance than the shading technology itself, underscoring the importance of developing optimized control algorithms.

- Wienold, J., **Sabeti, M.** and Lo Verso, V.R.M. (2025) "Do CIE-recommendations for proper light at the proper time conflict with glare?". *CIE Conference*, Vienna, Austria, July 2025.

  Abstract. CIE recently issued a position statement advocating for appropriate lighting at the right time specifically recommending a melanopic EDI of 250 lx at eye level during daytime. However, the statement also cautions that avoiding glare from windows requires "advanced lighting design guidance", implying a conflict between achieving healthy lighting and managing daylight-induced glare.

  This study examines whether such a conflict is justified.

  Both a theoretical analyses and results of a user study conducted at six locations suggest otherwise: recommended illuminance levels for healthy lighting are significantly lower than typical glare thresholds. In fact, vertical illuminance levels between 250 and 1000 lx from daylight typically reduce perceived glare from façades. A

supporting simulation study across three European climates, using typical shading devices and controls, further confirms this finding. The results demonstrate that healthy daytime lighting through daylight does not inherently increase glare risk and can be achieved without compromising visual comfort.

Acknowledgement

This thesis would not have been possible without the guidance, encouragement, and friendship of many wonderful people.

First and foremost, I owe my deepest gratitude to Dr Jan Wienold at LIPID, EPFL for his patient mentorship. Your readiness to entertain my endless questions and nurture my curiosity has shaped both this work and my growth as a researcher. I am grateful to Professor Valerio Lo Verso, whose enthusiasm for building physics first sparked my passion for the topic from my Bachelor, a passion has become more and more up to now.

I would like to also thank Hanieh Khodaei Tehrani, who helped me in this project and ensured I had a confident start. I also wish to acknowledge everyone in the LIPID lab; our informal conversations and shared laughter were a constant source of energy and fresh perspective. In particular, Prof. Maryline Andersen, your inspiring leadership, warmth, and understanding created an environment where this research—and I—could thrive.

Beyond academia, I am deeply grateful for my partner, whose unwavering belief in me has strengthened my confidence at every stage of this journey. thank you for reminding me of the bigger picture. Your support and love have been my anchor, grounding me through every challenge. Finally, heartful thanks to my family for their faith in my abilities and potentials.

To all of you, I extend my sincere appreciation.

Contents

List of Figures

List of Tables

Chapter 1

Introduction

1.1 Background and Motivation

Over the course of my studies and initial explorations into façade engineering and design, I've come to appreciate shading systems not merely as accessories to a building's envelope but as pivotal tools that shape how occupants experience and interact with their external environment. From the dramatic overhangs of classical Mediterranean villas to the finely tuned motorized louvers of today's smart façades, shading devices have always served dual purposes: to temper the harshness of direct sunlight and to sculpt the quality of light that penetrates interior spaces. In office contexts—where visual tasks dominate much of the day—the ability to finely control glare, contrast and daylight distribution becomes especially critical, not only for productivity but for long-term well-being.

As climate concerns intensify and the built environment's energy footprint comes under ever-closer scrutiny, shading systems have emerged as a frontline strategy in the battle to reduce heating, cooling and lighting loads. Advances in building performance simulation have revealed that appropriately configured shading can cut annual energy consumption significantly, yet these simulations also underscore a key lesson: no two climates behave the same. What offers optimal solar protection in a Mediterranean climate may prove inadequate in the tropics or overkill in temperate zones. This climate-specific complexity is, to me, both a challenge and an invitation—one that motivates the comparative scope of my thesis.

Beyond pure energy considerations, I'm especially intrigued by the nuanced role shading plays in human comfort and health. Light does more than illuminate: it entrains our circadian rhythms, influences mood, and even affects cognitive performance. Modern shading systems—whether roller fabrics or tinted glazing—hold the promise of balancing energy savings with dynamic daylight modulation that supports occupants' visual and non-visual needs. Exploring this intersection between different performance metrics feels to me like a largely overlooked area that demands thorough investigation.

Another trend that I find compelling is the shift from manual to automated—and now to hybrid—control regimes. Classic blinds offered manual adjustment but often suffered from suboptimal usage patterns: either left open when they should have been closed or closed at the wrong times, undermining their potential. Conversely, fully automated electrochromic systems promise precision but may lead to user dissatisfaction if occupants feel they lack control. My thesis seeks to bridge this divide by evaluating not only how these systems perform under automated control with manual override.

Thus, with the title "The impact of shading systems on indoor comfort and energy-

efficiency for offices: Comparative analysis of fabric roller blinds and electrochromic glazing under automated and manual controls," I aim to weave together these threads—architectural heritage,sustainable architecture, climate adaptation, human health and hybrid control strategies—into a cohesive study. By systematically comparing two leading dynamic and responsive shading technologies under automated and manual control across diverse climates, my goal is to provide valuable results that architects and practitioners can use to design façades and shadings that are as responsive to the needs of buildings as they are to the people within them.

Finally, by translating those performance differentials into clear metrics, the study contributes to the sustainability agenda that now frames contemporary design practice. The results establish quantitative links between shading choice, and occupant-centric daylight quality, furnishing architects with evidence they can apply during early concept stages to satisfy precise energy codes and green-rating criteria. By streamlining the iterative exchange between early façade design decisions and holistic building-performance modelling, the thesis enables shading strategies to be coordinated more effectively with other renewable-ready systems—an essential step toward meeting global sustainability goals.

1.2 Literature Review

In recent years, the integration of dynamic shading and facade technologies, such as electrochromic glazing and fabric roller blinds, has emerged as an effective strategy for enhancing energy efficiency while addressing occupant comfort in offices. Based on a systematic review and bibliometric analysis from the last five-year research, from 2019 to 2023, on dynamic facades, they were shown to deliver simultaneous improvements in thermal comfort, energy efficiency and daylight performance across every climate band surveyed [1]. Their climate-zone meta-analysis indicates that temperate locations show the greatest increases in daylight autonomy, whereas hot-arid regions achieve the largest cooling-energy reductions.

Complementing these findings, Garkuwa Jamilu et al. (2024) propose a comprehensive classification scheme for dynamic façades, synthesising insights from 26 international case studies across diverse climates. They demonstrate that smart materials and automated control systems can optimise daylighting, heat gain and natural ventilation—resulting in energy savings of up to 50 % and CO_2 emission reductions of up to 40 % compared to traditional static façades. Their typology distinguishes between passive, active and intelligent façades based on driving mechanisms (e.g. thermally responsive materials, sensor-actuated louvers or algorithm-driven skins), and they underscore the critical importance of techno-economic analyses that account for lifecycle costs and long-term operational resilience under real-world stresses [2].

Building on the growing body of evidence, Wang et al. (2024) carried out a focused systematic review that maps dynamic-façade technologies by both form and function. They group the solutions into four broad families—movable external shades, switchable or "smart" glazing, kinetic envelope skins, and ventilated double façades—and collate performance data drawn from on-site measurements as well as simulation studies. Across temperate climates, they report that well-configured dynamic façades can trim annual heating-plus-cooling energy by as much as 40 % while boosting daylight autonomy by 50–70 %. The review stresses that control strategy is the dominant variable: traditional rule-based controls recoup only about half the savings achieved by predictive or machine-learning algorithms that react continuously to weather forecasts and occupancy. Wang et al. also expose key knowledge gaps—most notably the shortage of long-term, full-scale monitoring campaigns and the absence of harmonised metrics for side-by-side comparison—arguing that common testing protocols and in-situ validation are prerequisites for moving dynamic façades from promising prototypes to reliable, market-ready products [3].

Alkhatib et al. (2021) present a comprehensive reviewn of adaptive façades, treating the building envelope as a multifunctional "skin." Their survey spans both opaque walls and glazed elements and highlights four core capabilities: harvesting energy via integrated PV/PVT laminates and solar-thermal collectors; regulating heat and mass transfer through switchable insulation layers, phase-change materials, or ventilated cavities; driving or tempering airflow with kinetic louvers and breathing panels; and shaping interior daylight with electrochromic, thermochromic, or mechanically actuated shading. Because these services are required at different moments, the authors stress the importance of systems that are reversible, durable, and capable of rapid response—pointing out that electrochromic glazing can tint within seconds, whereas phase-change materials may need hours to shift state. They contend that the principal performance bottleneck now lies in control rather than hardware. Although most buildings still rely on simple rule-based logic, research is pivoting toward hybrid strategies that combine predictive models with data-driven or

evolutionary algorithms. Machine-learning controllers that adapt to occupancy patterns and weather forecasts can unlock far greater energy savings, an imperative given that façades influence roughly 40 % of the global energy used for heating, cooling, lighting, and ventilation. Enabling such intelligent control, however, demands a basic suite of sensors—measuring outdoor irradiance and temperature, indoor temperatures, CO_2 or VOC levels, occupancy, and actuator positions—so that comfort goals are satisfied while energy demand is minimised [4].

Fabric shading systems are commonly used worldwide as a solution for regulating solar gains and mitigating glare in office settings. Building on human-centered evaluations, Karmann et al. (2023) conducted a semi-controlled office-like experiment to tease apart how fabric openness and colour jointly influence glare protection, view clarity and occupant behavior. In a west-facing mock-up, 32 participants experienced direct sun at three typical solar positions (morning, noon, afternoon) behind four neutrally coloured roller fabrics—light-gray and charcoal variants at low openness (1 %–3 %) and moderate openness (6 %–7 %). Participants rated discomfort glare on a nine-point scale and assessed view satisfaction, while their blind-adjustment actions were logged. According to the glare-control versus view-quality trade-off, fabrics with OF < 3 % virtually eliminated direct-sun glare (mean glare score ≤ 1) but scored below neutral on view satisfaction, as measured by both the EN 14501 glare classifications and the newer view-clarity index. Conversely, charcoal fabrics with OF > 6 % afforded a clear external view—participants reported an average 10° sightline—yet incurred moderate glare (mean scores around 3–4). Occupant override behavior shows that despite slightly higher glare under the more open fabrics, 75 % of participants voluntarily raised the blind by approximately 15 % to regain daylight and view access, mentioning "more light" and "visual connection to the outdoors" as primary drivers. Importantly, this modest lift did not significantly worsen glare perception, underscoring how even small overrides can rebalance comfort outcomes without compromising glare control. These results highlight the necessity of selecting fabric properties not only for their static shading performance but also for how they interact with real occupant behavior—findings that are critical for designing control schemes which accommodate user adjustments while maintaining overall visual comfort [5].

Bavaresco et al. (2019) used whole-building simulations in EnergyPlus to tease apart how both the logic that drives blind movements and the finish of the blind surface jointly influence cooling-energy demand. They defined three prototypical control schemes—time-based control (scheduling blind closure and opening based on self-reported occupant adjustment times); temperature-threshold control (closing the blinds when the indoor operative temperature exceeded 24 °C); and irradiance-threshold control (deploying blinds whenever incident solar radiation surpassed a set level). Each control pattern was paired with two internal-blind finishes: a conventional fabric (higher emissivity) and a low-emissivity metallic coating. Simulations covered a matrix of room orientations (north, east, south, west), window-to-wall ratios (20 %, 50 %, and 80 %) and room aspect ratios. Their results reveal that blind finishing matters: metallic blinds reduced annual cooling-energy consumption by up to 12 % compared to fabric blinds, especially in west-facing zones with high solar exposure. Control pattern interacts with material; for example, irradiance-based controls yielded the largest savings when paired with metallic finishes, leveraging the metal's reflectivity to deflect solar gains before they enter the space. Trade-offs in user-aligned strategies show that time-based control with fabric blinds produced more modest savings, yet closely followed typical occupant adjustment habits. Together, these findings demonstrate that accurately modelling cooling loads in offices requires careful

specification of both the blind's physical properties (solar absorptance, thermal emissivity) and the algorithm driving its operation [6].

Lu et al. (2024) present a measurement-aided Radiance workflow that tightly couples a roller shade's openness factor (OF) and visible transmittance (VT) with annual, image-based Daylight Glare Probability (DGP) metrics. Their method proceeds in three steps: (1) BSDF characterisation—rather than rely on generic material libraries, they first measure the shade's bidirectional scattering distribution function using a peak-extraction algorithm to capture both specular and diffuse transmission components; (2) Radiance simulation—they run full-year, hourly Radiance five-phase simulations under a Perez sky model for a prototypical office space, generating luminance maps for each hour and view direction; (3) Image-based DGP evaluation—using `evalglare`, they calculate DGP directly from these images, yielding a high-fidelity discomfort-frequency profile. Shade-performance curves were developed for south- and west-facing offices in Chicago, Los Angeles and Hong Kong — both window-facing and side-view — mapping allowable combinations of visible transmittance without glare (Tv,n-n) and with high-angle glare (Tv,n-h) that keep annual discomfort glare below 5 % of occupied hours. The non-linear boundaries reflect a trade-off between contrast glare (worse with dark fabrics) and adaptation glare (worse with light fabrics), yielding location- and orientation-specific tipping points. For instance, west-facing offices require tighter Tv,n-n limits—especially in LA (< 1.4 %)—due to low-sun afternoon glare, whereas side views tolerate higher values (Tv,n-n < 5 %, Tv,n-h ≤ 20 %) since glare hits beyond fabric cut-off angles. These climate- and orientation-specific maps offer practitioners clear upper bounds for selecting roller-shade products: by choosing OF and VT within the recommended envelope for their façade orientation, designers can balance glare protection with daylight provision without resorting to iterative trial-and-error simulations [7].

Building on these insights, Fathi and Kavoosi (2021) developed a detailed annual simulation model of a 20-storey office tower to quantify how electrochromic glazing—and its integration with other envelope and systems technologies—impacts whole-building energy use across four Iranian climate zones (cold, temperate, hot-arid and hot-humid). They first isolated the effect of EC windows versus conventional clear and low-E double glazing, finding that with indoor-air-temperature control the energy-saving potential is between 13 and 14 %, while this saving is around 11–12 % with outdoor-air-temperature control in all climates. However, the solar-control strategy shows different percentages of energy savings in different climates: this control shows the highest energy saving (13.44 %) in temperate climates and the lowest (8.55 %) in hot-humid climates. Next, they defined 12 combined scenarios—pairing EC glazing with optimal glazing types, building-integrated photovoltaics (BIPV) modules and an advanced building-energy-management system (BEMS). Under the most comprehensive package (EC + BIPV + BEMS), simulations showed up to 35.6 % drop in annual energy consumption. Importantly, they benchmarked their model against measured data and report simulation–measurement deviations of just 1.6–6.2 %, underscoring both the robustness of their approach and the real-world applicability of EC technologies for energy-intensive office buildings [8].

Al-Fasi and Budaiwi (2023) set up a full-year, hourly simulation of a multi-zone office building in Dhahran using DesignBuilder (EnergyPlus engine) to investigate how EC smart windows perform against conventional double low-E glazing. The model replaced all existing windows with five-layer EC glazings and equipped each daylit zone with ceiling-mounted illuminance and glare sensors. A daylight control strategy was implemented, and the glazing modulated its visible transmittance between 13 % (tinted) and 75 % (clear) to

balance daylight admission, solar heat gain and visual comfort. Under the daylight-trigger strategy, EC windows cut total annual lighting energy by an additional 25 % and cooling energy by 9 %. The glare-trigger achieved 12 % lighting and 14 % cooling savings. Their findings demonstrate that, in a hot-humid context, daylight-only triggers maximise energy savings but risk occupant discomfort, whereas glare-based control strikes a more balanced compromise—delivering substantial energy reductions without sacrificing visual comfort. This dual-trigger comparison provides a clear precedent for selecting EC control schemes that align with both sustainability goals and user well-being in demanding climates [9].

Building on these case-study findings, Tabet Aoul et al.'s state-of-the-art review synthesises the broader performance, design and market challenges for electrochromic glazing. The authors categorise electrochromic materials into different systems, comparing their coloration efficiencies, switching speeds and cycle lifetimes. Across simulated and field studies, EC glazing is shown to reduce annual electricity demand by 7–8 % for moderate window-to-wall ratios and by 14–16 % for large glazing areas. When broken down by building type, savings range from 6–11 % in commercial offices to 8–15 % in residential settings. Despite clear benefits, the authors point to persistent hurdles: colour neutrality (many electrochromic tints exhibit blue or amber hues), switching latency (especially under low-temperature conditions), long-term durability (performance degradation under UV exposure and humidity) and high upfront costs relative to conventional static glazing. By charting these technical trade-offs and commercial constraints, the review frames the path forward for electrochromic glazing: improving material lifetimes, accelerating response times and integrating with other façade systems to unlock broader deployment in low-energy buildings [10].

While both fabric blinds and EC glazing have been extensively studied in isolation, direct comparisons in office environments remain limited. A recent comparative investigation by Alkhatib et al. (2023) directly compared EC glazing and roller blinds in a Dublin-climate office model, applying seven different control algorithms to each façade type—namely rule-based logic, proportional–integral–derivative (PID), anti-windup PID, and a model-predictive controller (MPC) among others—to drive shading actions. By matching all other envelope and HVAC parameters, they isolated the impacts of both the control strategy and the physical switching behavior (continuous tinting vs. discrete blind positions) on annual energy loads and daylight-comfort outcomes. Under rule-based and PID schemes, treating an electrochromic window as an "equivalent roller blind" led to notable over-estimations of building-energy consumption (heating + cooling + lighting) and inflated predictions of daylight-discomfort hours—errors the authors attribute to the blind's binary open/close behavior failing to mimic the EC's fine-tuned transmittance profile. By contrast, the MPC approach—leveraging weather forecasts and occupancy patterns—minimised these discrepancies: energy-use predictions for the two façade types converged closely, and simulated daylight-comfort metrics aligned within a few percent. These findings underscore that control-algorithm fidelity, as much as optical modelling accuracy, is pivotal when benchmarking dynamic façade technologies in office simulations [11].

Building on these converging insights, the present study addresses several critical gaps identified in the literature. Few studies have evaluated both electrochromic glazing and fabric blinds under identical automated algorithms with manual override. We therefore implement an automated control with manual override, ensuring that our framework captures real-world interactions alongside algorithmic actions. Second, we extend performance metrics by integrating energy demand, daylight provision, glare perception and non-visual potential indicators. Simulations span three representative European climates—Northern

European (Stockholm), Central European (Frankfurt) and Southern European (Rome). Third, we consider two different configuration of fabric blinds and window glazing (internal fabric blinds + solar control glazing , external fabric blinds + lowE glazing) based on the previous literature:

Khalaf et al. (2019) carry out a parametric simulation of a prototypical Istanbul primary-school façade to rank sixteen glazing–shading pairings. Among the tested options, the stand-out performer is a double low-E insulated glass unit fronted by a 0.5 m exterior louvre/roller blind: the low-emissivity coating trims conductive heat losses in winter, while the blind intercepts most short-wave gains before they reach the pane. Together, the two measures slash total annual energy use by roughly 8 % and cut heating demand by about 15 % relative to the baseline of clear double glazing without shading; cooling peaks also drop far enough to resize HVAC equipment. Khalaf's team further cites the *ASHRAE Fundamentals* benchmark that a well-designed glazed-and-shaded façade can block up to 80 % of incident solar heat, underscoring why the low-E + external-blind strategy consistently outranks clear glass or interior devices in their matrix of results [12].

Singh et al. (2015) examine four double-glazing types in combination with high-permeability woven roller shades for an office in the cool, overcast climate of Shillong, India. Their integrated daylight-and-thermal simulations reveal that a spectrally selective solar-control double pane ($U \approx 1.6$ W m^{-2} K,SHGC ≈ 0.21,$\tau_{\mathrm{v}} \approx 0.30$) delivers the best year-round outcome: left bare in winter to harvest passive solar gains, then paired with the roller shade in summer to curb glare, it achieves the highest annual energy-saving potential, maintains ≥ 50 % glare-free occupied hours, and boosts useful daylight illuminance to 53–88 % across orientations. High-SHGC clear glass, by contrast, forces much deeper shade deployment and erodes the lighting-energy benefit. The study therefore recommends coupling internal blinds with inherently solar-filtering glass so the shade can concentrate on fine-tuning daylight rather than blocking heat[13].

In a study by Tzempelikos et al. (2007) they push the analysis further by embedding a dynamic roller shade into a coupled daylight–thermal simulation of office perimeter zones. Varying window-to-wall ratio, shade openness and automatic control logic, they show that an exterior shade automatically deployed to maintain 100–500 lx of daylight can simultaneously cut cooling energy by up to 37 % and lighting electricity by 10–20 % compared with an unshaded clear window—without sacrificing visual comfort. The authors stress that such gains materialise only when shading design, glazing properties and daylight-responsive lighting controls are optimised as a single system; static blinds or manual control leave most of the savings untapped [14].

In another study the author blends laboratory calorimetry with ParaSol v2.0 simulations to compare external and internal shading on Swedish office windows. His measurements confirm that external blinds or awnings almost halve both peak and annual cooling loads, whereas internal roller or Venetian blinds achieve only about a one-third reduction under identical conditions. Parametric sweeps further reveal that the cooling-load benefit of interior blinds doubles when they are combined with low-absorption, solar-control glazing, highlighting the importance of matching blind reflectance with glass absorption. The thesis also introduces a novel incidence-angle model for g-values of asymmetric shades, later adopted in EN 14500 [15].

Kuhn et al. (2014) also addresses a critical measurement gap by refining steady-state calorimetric methods for determining the solar-heat-gain coefficient (g-value) of complex glazing-plus-shade assemblies. Drawing on 25 years of Fraunhofer ISE experience, the paper details two indoor set-ups—cooled absorber plate and cooled box—that achieve ±3 %

accuracy across orientations and dynamic configurations. It also provides correction algorithms that translate laboratory results to ISO 9050 reference conditions, giving façade engineers a robust, standard-compatible path to quantify how much combined systems such as solar-control glass with an internal blind actually reduce solar gains (measured $g \approx 0.19$–0.22 versus ≈ 0.36 for the same blind on clear glass). These verified data underpin simulation inputs and rating schemes for advanced window attachments worldwide [16].

Moreover, this study considers different openness factors, colours and surface emissivities for fabric blinds and comparing them with blue-tinted electrochromic glazing which is the most typical based on the previous literature. Kraft (2024) retraces four decades of research on Prussian-blue electrochromics and explains why the intense royal-blue tint is still the default for large-area smart windows. Prussian blue is a low-cost, deep-blue pigment whose iron atoms can toggle between two charge states (Fe^{III}/Fe^{II}) That simple redox switch creates a broad light-absorption band centred near 700 nm. As a result, a very thin film (about 200 nm) can go from letting in light to blocking roughly half of the visible spectrum when you apply less than 2 V. The transition is fast—just a few seconds—and the coating can cycle on and off well over a million times with little wear. No other inexpensive electrochromic "colour" yet offers the same mix of large visible-light modulation, low driving voltage, high durability, and modest material cost, although its strong blue tint can slightly distort colour rendering [17].

According to Niklasson & Granqvist (2007), tungsten trioxide (WO_3) is the leading oxide for electrochromic "smart-window" coatings: a small electric bias inserts Li^+ ions into its lattice, turning an otherwise transparent film a deep blue with a coloration efficiency of ~ 50 cm^2 C^{-1}. The material resists UV degradation and is compatible with inexpensive sputter deposition, and—when paired with a nickel-oxide counter electrode—the glazing can switch from almost fully clear to about one-tenth that brightness (an 8–10:1 transmittance swing), easily meeting modern daylight- and glare-control targets that brown, grey, or green chemistries still struggle to satisfy [18].

Scaling from materials to whole buildings, Wu et al. (2023) catalogue more than 200 field and simulation studies and note that "electrochromic bleached states have higher transmittance, while tinted states are mostly blue". Because both canonical WO_3 and Prussian-blue mechanisms converge on a cool-blue hue, the authors argue this tint balances solar-heat-gain reduction, acceptable colour rendition (CRI > 80) and occupant preference—explaining why leading brands such as SageGlass and View continue to ship blue-tinted products despite ongoing work on neutral-grey formulations [19].

Finally, this comprehensive approach not only benchmarks electrochromic glazing and fabric blinds on an equal footing but also equips designers and facility managers with actionable criteria for selecting and deploying dynamic façade solutions tailored to the climatic and behavioural realities of modern office buildings.

Chapter 2

Methodology

2.1 Climatic Overview

Façade technologies such as electrochromic glazing and fabric blinds cannot operate effectively in isolation; their thermal, optical, and daylight responses are tightly coupled to outdoor conditions. A rigorous, climate-specific baseline is therefore beneficial if we are to evaluate their behavior accurately and to draw conclusions that remain valid beyond a single site. To capture the extent of European weather realities, this study compares three distinct climate zones—Central (Frankfurt, Germany), Northern (Stockholm, Sweden), and Southern (Rome, Italy). Each location brings a unique mix of climatic conditions. The climatic indicators outlined in the following sections have been selected solely for their relevance to the façade control algorithms developed later.

2.1.1 Global horizontal radiation

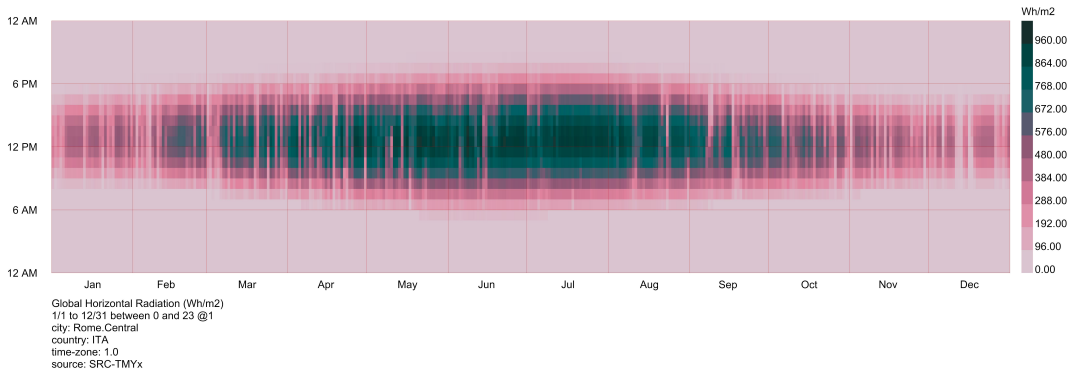

(a) Rome (Southern Europe).

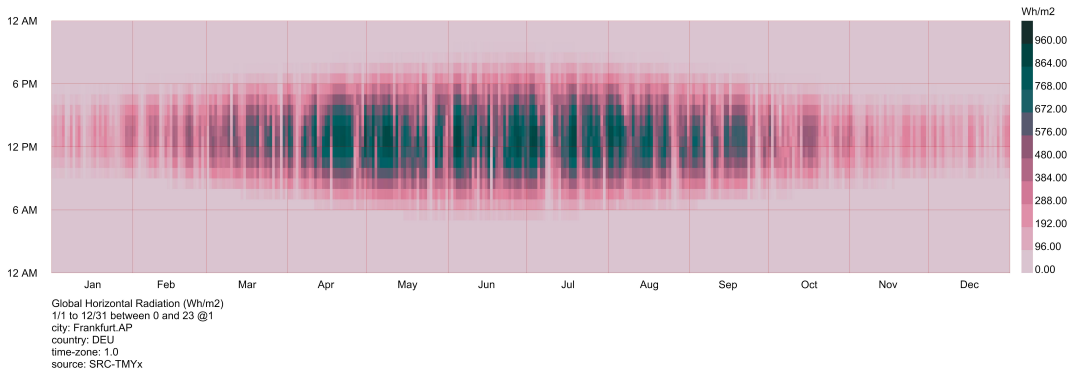

(b) Frankfurt (Central Europe).

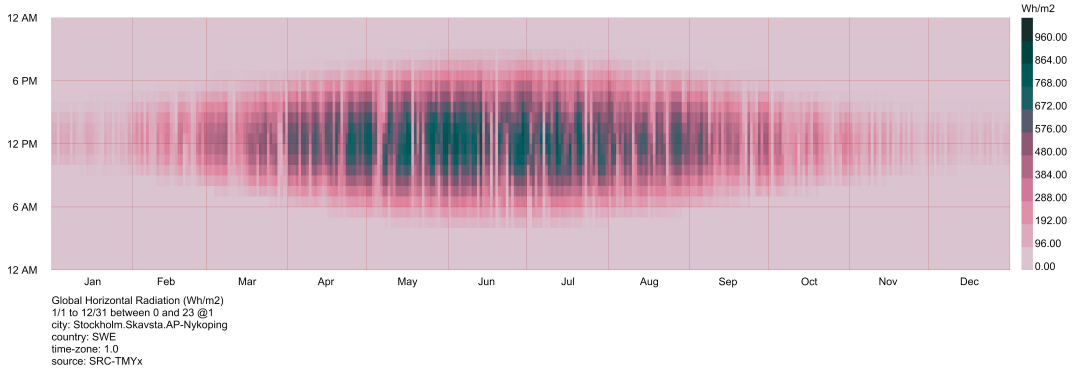

(c) Stockholm (Northern Europe).

Figure 2.1: Annual global horizontal irradiance (GHI) profiles for the three study climates.

Based on the fig. 2.1, the key comparative points are:

Peak Irradiance & Sun Angle.

Rome, due to its lower latitude and typically clearer summer skies, experiences the highest noontime peak irradiance, reaching approximately 960 Wh/m^2. Frankfurt, situated at a mid-latitude, falls in between with peak irradiance values around 870 Wh/m^2. Stockholm, by contrast, has the lowest maximum values, peaking near 800 Wh/m^2, which are limited by a lower solar elevation even at midsummer.

Winter Insolation & Daylength.

During winter, Rome retains moderate solar availability, receiving around 100–200 Wh/m² at noon over roughly 10 hours of daylight. Frankfurt also benefits from meaningful winter peaks, with irradiance around 100–150 Wh/m² at noon and about 8 hours of daylength. Stockholm, however, experiences very low winter radiation levels—often under 50 Wh/m²—accompanied by short days of approximately 6 hours. This significant limitation implies a need for alternative or storage strategies during the darkest months from November to January.

Summer Daylength vs. Variability.

Rome demonstrates highly favorable summer conditions, with long periods of clear skies and daylight ranging from 10 to 15 hours. This results in stable, high midday irradiance and reliable solar output. Frankfurt sees about 16 hours of daylight, which, combined with moderate cloudiness, leads to relatively stable summer performance, albeit less extreme than Rome. In Stockholm, summer days stretch to around 18 hours, but frequent cloud cover reduces average hourly irradiance outside of the noon peak, moderating overall solar gains despite the extended daylight.

In table 2.1, the summary of the main features is presented.

Table 2.1: Global horizontal radiation, Main features of the three climates

Feature	**Rome**	**Stockholm**	**Frankfurt**
Latitude Approx.	41.9° N	58.8° N	50.0° N
Daylength (Mid-winter)	≈ 10 hr (07:00–17:00)	≈ 6–7 hr (08:30–15:30)	≈ 8 hr (08:00–16:00)
Daylength (Mid-summer)	≈ 15 hr (05:00–20:00)	≈ 18 hr (03:00–21:00)	≈ 16 hr (05:30–20:00)
Max Global horizontal radiation (Wh/m^2)	∼ 960 (June–July at noon)	∼ 800 (June at noon)	∼ 870 (June–July at noon)
Summer Radiation Pattern	Broad, contiguous high-irradiance core (10:00–15:00) with many clear days	Extended dawn–dusk band (04:00–22:00) but patchy due to frequent clouds	Midday plateau (10:00–15:00) moderately intense, with some cloud interruptions
Winter Radiation Pattern	Midday ∼100–200 Wh/m^2 on clearer days (≈ 10 hr of low-level sun)	Virtually zero (< 50 Wh/m^2) except a narrow midday spike (≈ 3 hr)	Midday ∼100–150 Wh/m^2 over ≈ 8 hr of daylight
Seasonal Transition	Early ramp-up: spring noontime > 400 Wh/m^2 by March; autumn declines after September	Compressed: spring peaks only by late April/May; autumn drops by August/September	Gradual: spring ∼500–600 Wh/m^2 by April; autumn similar decline by September
Day-to-Day Variability	Lowest in summer (sustained clear skies); moderate in shoulder months	Highest year-round (rapid cloud cover changes even in summer)	Moderate variability (clouds more frequent than Rome but less than Stockholm)

2.1.2 Outdoor temperature

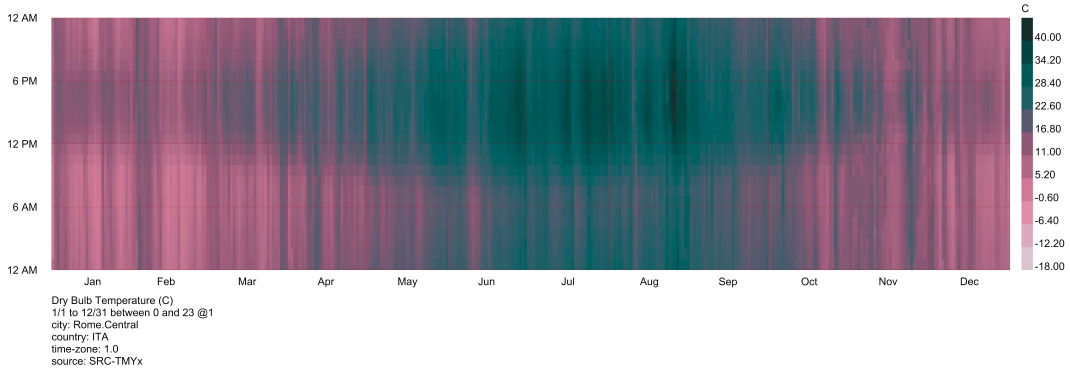

(a) Rome (Southern Europe).

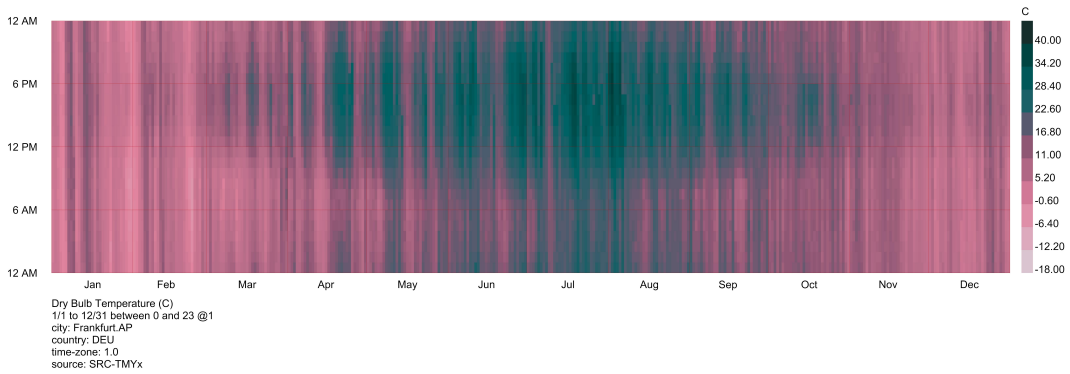

(b) Frankfurt (Central Europe).

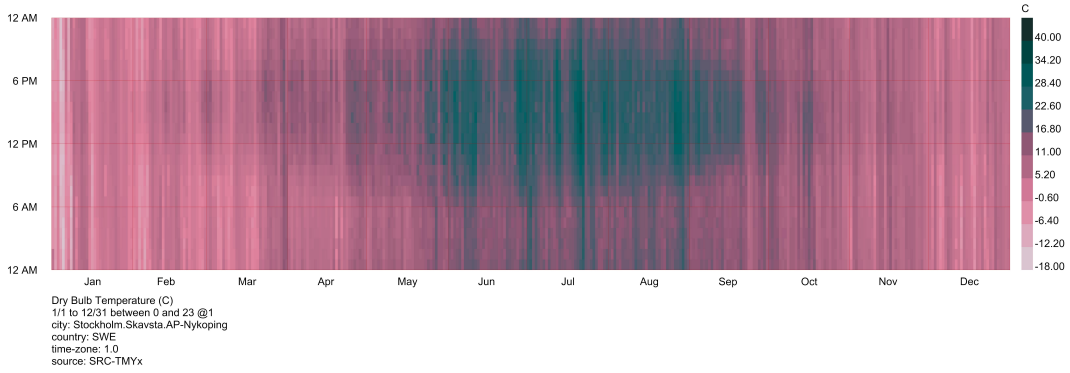

(c) Stockholm (Northern Europe).

Figure 2.2: Annual outdoor dry-bulb temperature profiles for the three study climates.

Winter Severity

According to fig. 2.2, Winter conditions vary significantly across the three cities. Rome experiences the mildest winters, with nighttime lows typically ranging between -1°C and 2°C and daytime temperatures reaching 8–15°C. Frost is minimal in this southern climate. Frankfurt, located further north, faces colder winters, where nighttime temperatures can drop to -8°C, and daytime values usually range between 0°C and 8°C, with a moderate potential for snowfall. Stockholm endures the harshest winters among the three, with night-

time lows frequently falling between -18°C and -10°C. Even during the day, temperatures often remain below freezing, typically ranging from -10°C to 0°C.

Summer Heat

During summer, based on fig. 2.2, Rome becomes quite hot, with daytime temperatures peaking between 30°C and 40°C, and nighttime values rarely dropping below 15°C. Frankfurt also experiences hot summers, with daytime highs ranging from 25°C to 36°C. However, its nights are somewhat cooler than those in Rome, falling between 12°C and 18°C. In contrast, Stockholm has warm but generally milder summers, with daytime temperatures typically between 20°C and 30°C and cooler nights ranging from 10°C to 15°C.

Diurnal & Seasonal Variability

The degree of both seasonal and daily (diurnal) temperature variation also differs across the locations as represented in fig. 2.2. Rome shows moderate diurnal fluctuations—ranging from about 10°C to 20°C—and a seasonal temperature span of roughly 40°C. Its climate benefits from Mediterranean moderation, resulting in more gradual transitions between seasons. Frankfurt exhibits a moderate seasonal range of around 45°C and diurnal swings of about 10–15°C year-round, offering smoother thermal transitions than those experienced in Stockholm. Stockholm stands out with a large seasonal temperature swing, often reaching up to 50°C, and notable diurnal shifts of 10–15°C during winter. The city also undergoes rapid and often abrupt transitions during spring and autumn.

Day-to-Day Variability

On a day-to-day basis, the fig. 2.2 shows that Rome tends to remain relatively stable, with only occasional cold snaps or heat waves disturbing an otherwise consistent pattern. Frankfurt, in line with broader Central European trends, displays moderate variability, with occasional weather fronts triggering sudden changes in conditions. Stockholm, however, is characterized by high variability throughout the year, frequently experiencing abrupt cold snaps or heat spikes regardless of the season.

In table 2.2, the summary of the main features is presented.

Table 2.2: Outdoor temperature, Main features of the three climates

Feature	**Rome**	**Frankfurt**	**Stockholm**
Latitude (approx.)	41.9°N	50.0°N	58.8°N
Winter min temp (°C)	−1 to 2 (night)	−8 to 0 (night)	−18 to −10 (night)
Winter max temp (°C)	8 to 15 (day)	0 to 8 (day)	−10 to 0 (day)
Summer min temp (°C)	15 to 20 (night)	12 to 18 (night)	10 to 15 (night)
Summer max temp (°C)	30 to 40 (day)	25 to 36 (day)	20 to 30 (day)
Diurnal variation (ΔT)	Moderate (10–20°C swing)	Moderate (10–15°C yr-round)	Large in winter (10–15°C); moderate in summer (10–15°C)
Seasonal range (ΔT)	≈40°C span	≈45°C span	≈50°C span
Day-to-day variability	Moderate; occasional cold snaps	Moderate; frontal swings	High; rapid shifts

2.1.3 Sun-up Hours

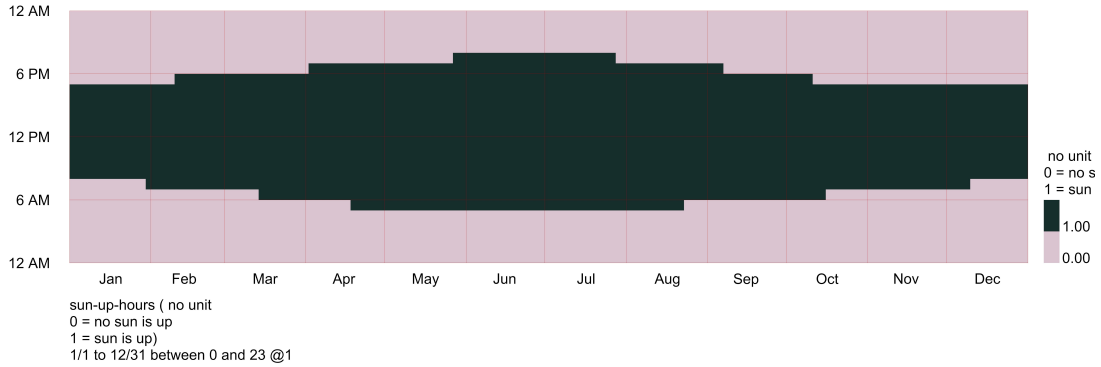

(a) Rome (Southern Europe).

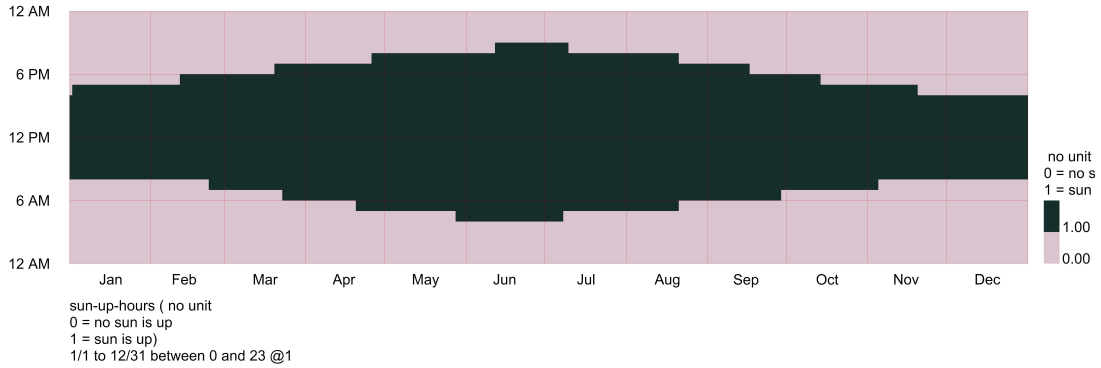

(b) Frankfurt (Central Europe).

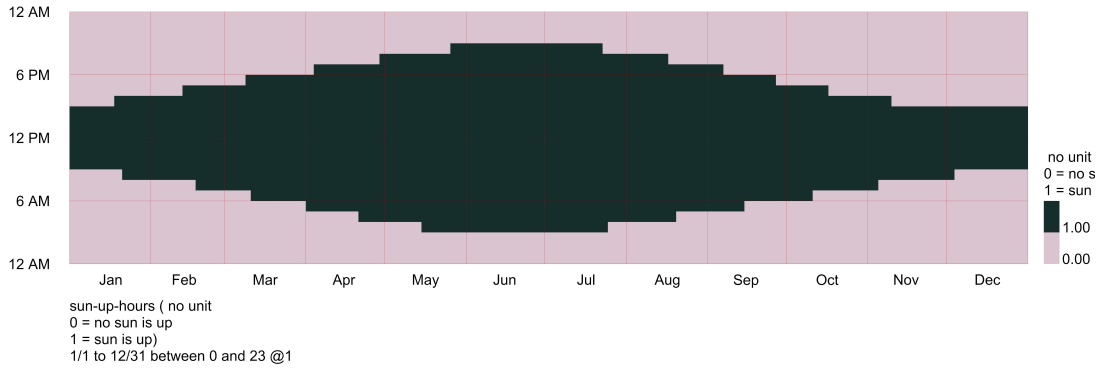

(c) Stockholm (Northern Europe).

Figure 2.3: Annual sunrise–sunset (sun-up) duration profiles for the three study climates.

based on fig. 2.3, the analysis of sun-up hours across the three cities reveals notable seasonal differences in daylength. During winter, Rome enjoys the longest duration of daylight among the three, with the sun rising around 07:00 and setting near 17:00—resulting in approximately 10 hours of daylight. Frankfurt experiences a moderate winter daylength, with sun-up occurring from roughly 08:00 to 16:00, totaling about 8 hours. Stockholm has the shortest winter day, with daylight lasting from around 08:30 to 15:30, giving only about 6 hours of sun-up.

In contrast, summer daylength is longest in Stockholm, where the sun rises as early

as 03:00 and sets around 21:00, providing about 18 hours of daylight. Frankfurt sees a summer sun-up window from approximately 05:30 to 20:00—about 16 hours in total. Rome, despite being farther south, has slightly shorter summer days than Stockholm and Frankfurt, with daylight spanning from around 05:00 to 20:00, resulting in about 15 hours.

In terms of diurnal consistency, Rome shows the most stable daylight changes throughout the year, with gradual and predictable shifts in sunrise and sunset times. Frankfurt demonstrates steady seasonal adjustments without extreme fluctuations. Stockholm, however, experiences the most dramatic changes, especially around the equinoxes, with rapid transitions in sun-up times and an extended period of near-continuous daylight during summer.

In the table below, the summary of the main features is presented.

Table 2.3: Sun-up Hours summary for the three study climates.

Feature	**Rome**	**Stockholm**	**Frankfurt**
Latitude Approx.	41.9° N	58.8° N	50.0° N
Midwinter Daylength	≈ 10 hr (07:00–17:00)	≈ 6 hr (08:30–15:30)	≈ 8 hr (08:00–16:00)
Midsummer Daylength	≈ 15 hr (05:00–20:00)	≈ 18 hr (03:00–21:00)	≈ 16 hr (05:30–20:00)
Day-to-Day Consistency	Fairly consistent sunrise/sunset shifts	Rapid shifts around equinoxes	Moderate shift pace year-round
Extreme Variability	Minimal (lower latitude)	Maximal (near-midnight sun)	Intermediate

2.2 Interior configuration and building envelope

Rhinoceros (Rhino) [20] and its visual-scripting plugin Grasshopper [21] form the core modelling environment. The building is first modelled in Rhino as a shoebox-shaped volume. Within Grasshopper, the Honeybee and Ladybug plugins [22] are used to assign the construction assemblies and boundary conditions to every surface. In this setup, only the façade that contains the window is classified as an exterior (outdoor) surface; all remaining faces are treated as adiabatic boundaries, representing an office room in a building.

2.2.1 Office geometry

In fig. 2.4, the office floor plan and section are illustrated to understnad better the general geometry.

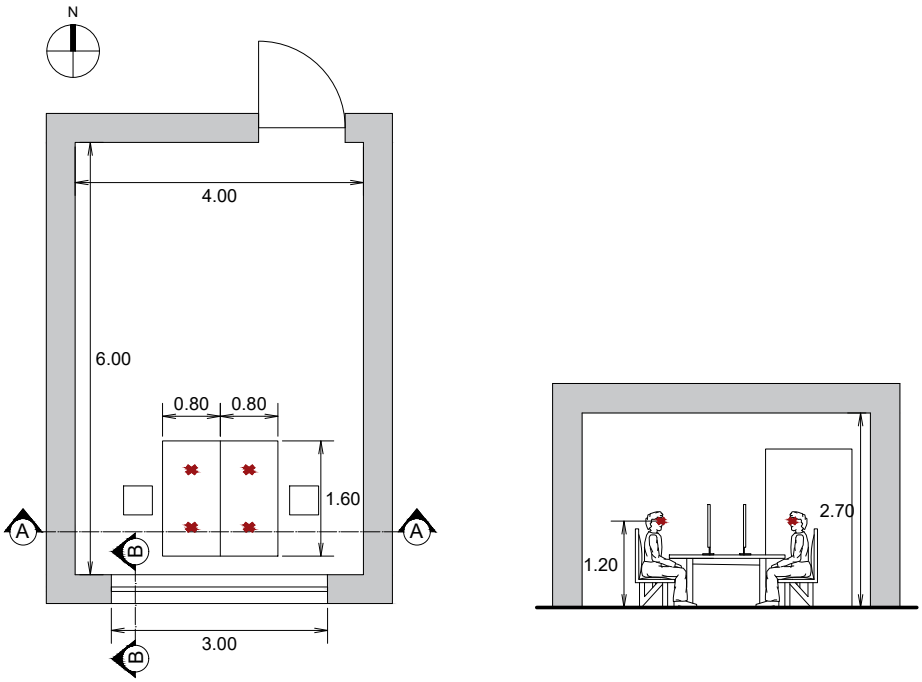

Figure 2.4: Left: Office Floor plan. Right: Section B-B (Dimensions in m)

2.2.2 Building envelope

Figure 2.5 represent the stratigraphy of building systems, including exterior wall, interior wall, interior floor and ceiling. For better understanding of the simulation set-up, they are drawn as the same version of stratigraphies that were implemented in Grasshopper for Energy simulation.

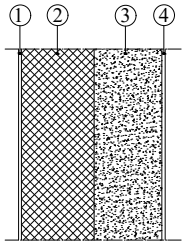

1. Exterior rendering with reinforcing mesh (t=0.008m , λ=0.9W/m.K , ρ=1700kg/m3 , c=1000J/kg.K)
2. EPS (Expanded Polystyrene Insulation) (t=0.21m , λ=0.04W/m.K , ρ=15kg/m3 , c=1400J/kg.K)
3. Reinforced concrete(with 1% steel) (t=0.2m , λ=2.3W/m.K , ρ=2300kg/m3 , c=1000J/kg.K)
4. Interior plaster (t=0.01m , λ=0.7W/m.K , ρ=1700kg/m3 , c=1000J/kg.K)

(a) Exterior wall.

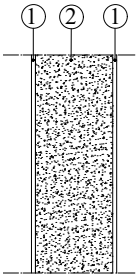

1. Interior plaster (t=0.01m , λ=0.7W/m.K , ρ=1700kg/m3 , c=1000J/kg.K)
2. Reinforced concrete(with 1% steel) (t=0.2m , λ=2.3W/m.K , ρ=2300kg/m3 , c=1000J/kg.K

(b) Interior wall.

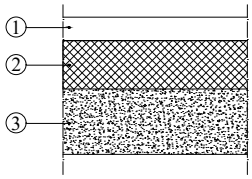

1. Floating screed (Ceramic/porcelain Tiles) (t=0.07m , λ=1.4W/m.K , ρ=2300kg/m3 , c=840J/kg.K)
2. EPS (Expanded Polystyrene Insulation) (t=0.145m , λ=0.04W/m.K , ρ=15kg/m3 , c=1400J/kg.K)
3. Reinforced concrete(with 1% steel) (t=0.2m , λ=2.3W/m.K , ρ=2300kg/m3 , c=1000J/kg.K)

(c) Ceiling/Floor.

Figure 2.5: Building envelope stratigraphies

2.2.3 Glazing and shading materials/setup

Three fabric types are examined in this study: black, pearl, and black-metallized—where the latter is a black fabric with a metallic coating applied to one side to enhance solar reflectance. Each fabric is evaluated with openness factors of 1% and/or 3%, which represent the proportion of open area in the fabric weave and thus influence both daylight transmission and visual connection to the outside. The optical and thermal properties used for these fabrics are based on synthetic data generated to reflect the characteristics of widely available commercial products. For the transparent and electrochromic glazing types, the spectral and optical properties are derived using the LBNL Window tool,

ensuring consistency and realism in material performance inputs [23].

The configurations for both fabric roller blinds and electrochromic glazing are depicted in fig. 2.6. The fabric roller blind system—whether mounted externally or internally—is designed to operate in four discrete deployment levels, corresponding to different blind heights, which are triggered based on sensor-driven activation signals. This allows for partial or full coverage of the window surface to respond dynamically to daylight and solar gain conditions. In the case of the electrochromic glazing, the system is configured with a vertical split, dividing the window into two independently controlled zones: the upper and lower panes. This zonal control strategy enables more refined modulation of daylight and glare by allowing the tint level of each section to be adjusted separately in response to environmental inputs or occupant needs. Moreover in table 2.4, the material properties of the different glazings and fabrics are represented.

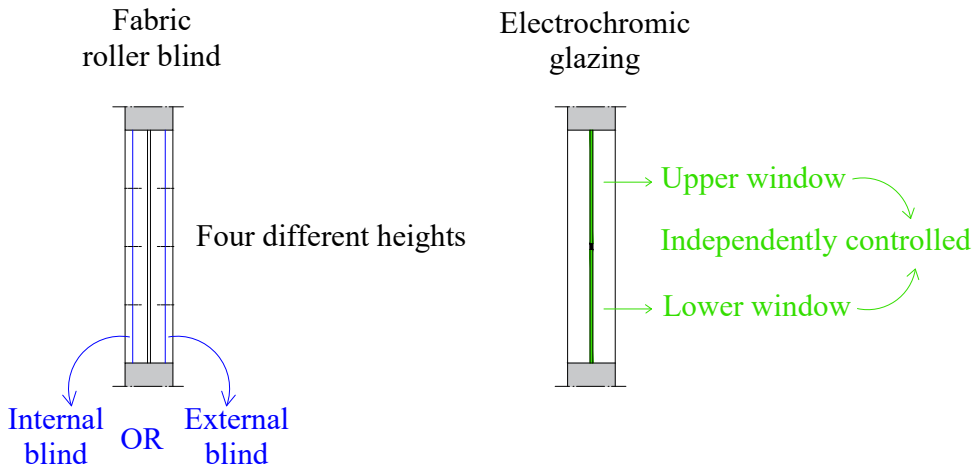

Figure 2.6: Glazing and shading setup

Table 2.4: Optical properties of the glazing and fabric layers.

	Fabric					**Glazing**					
Property	Black 1 %	Black 3 %	Pearl 1 %	Pearl 3 %	Metallised 3 %	Low-E	Solar control	State 0	State 1	State 2	State 3
OF [%]	1	3	1	3	3			*			
T_v [%]	1	3	9	9	3	78	59.4	56.6	34.3	5	1.2
T_s [%]	1	3	9	9	4	53	26	30.5	15	2	0.5
SHGC [%]			**			60.4	30.5	37	21.2	8.1	6.6

* The openness factor (OF) is not defined for monolithic glazing layers.
** For fabrics, SHGC is calculated for the fabric mounted on the reference solar-control glass.

2.3 Control schemes - during usage hours

Usage hours include the working days from 8 a.m. to 6 p.m., excluding the weekends as holidays. To detect and mitigate uncomfortable glare (direct sunlight striking an occupant's eyes or desk), we have modeled six virtual sensors around each workstation (see fig. 2.4). Four of these sensor arrays lie horizontally across the desktop, while two additional sensors are mounted vertically at eye height and oriented perpendicular view direction. Two shading technologies are compared. fabric roller blinds whose height is dynamically adjusted, and electrochromic glazing, which can modulate its tint in multiple levels. The fabric height adjustment enable comparison with EC which offers multiple tint levels. For EC, the overall window is split into an upper half and a lower half, each controlled independently. In the sections that follow, we will present the detailed control logic for each configuration, and discuss how each scheme balances glare prevention, daylight provision, and energy performance.

2.3.1 Solar control glazing + internal fabric blinds: Glare-avoidance control only.

This control scheme is based solely on glare-avoidance logic and is designed to emulate manual occupant behavior. where shading is triggered by glare metrics and solar exposure, mimicking occupant actions. As activation of the internal blinds has a minor effect on the overall g-value, Solar gain control was ineffective for this system, because it showed either no measurable reduction in cooling load or a slight increase. Such marginal energy effects do not justify the accompanying compromise on daylight performance, particularly because the glazing itself already provides solar-control properties. Shading activation is driven by two complementary glare metrics:

Glare Occurance

- An activation signal is triggered for the fabric blind when the Daylight Glare Probability (DGP) exceeds 0.35. DGP is the probability that an average occupant will experience discomfort glare produced by daylight within the visual field [24].
- **Control action.** If DGP > 0.35, the blind is lowered until DGP falls just below this threshold. Should DGP remain above 0.35 despite further lowering, the blind is held at the height at which DGP is minimised.

Direct Sun on the Desk

- A separate rule addresses glare caused by sunlight striking the work surface. Shading is triggered when *both* of the following conditions are met:

  (i) direct sunlight reaches any of the horizontal desk sensors;

  (ii) vertical façade irradiance E_{f} exceeds $450\,\mathrm{W\,m^{-2}}$.

- The $450\,\mathrm{W\,m^{-2}}$ threshold was determined by iterative testing to avoid excessive blind closures while still preventing high-contrast reflections and hotspots on the desk surface.

By combining line-of-sight glare detection with desk-level irradiance monitoring, this scheme closely mimics how an occupant might manually adjust blinds, only engaging

shading when and where it is truly needed to preserve visual comfort. The general control scheme is represented in table 2.5. The more detailed visualization of the control strategy is shown as a flowchart in fig. 2.7.

2.3.2 Low-E glazing + external fabric blinds: Glare-avoidance control and Solar-gain control

This control strategy includes the glare-avoidance logic described in section 2.3.1 with an additional control of solar-gain management, effectively operating in two distinct modes depending on prevailing façade irradiance and outdoor air temperature. The system switches into 'summer-mode' only when the seven-day average temperature indicates a risk of overheating ($>$ 17 °C: this value is also achieved based on the analysis of the temperature and its seven-day average in all three different climates in order to achieve a logical summer-mode period).

Glare-avoidance control

Follows exactly the same trigger rules as in section 2.3.1: monitoring direct sun in the occupant's view with a Daylight Glare Probability threshold of 0.35, and direct sun on the desk when vertical irradiance $E_f > 450$ W/m². When either of these conditions is met, the shading device responds by lowering the blind to the height that reduces glare below threshold, holding it there or at the minimum-glare height if the threshold cannot be met.

Solar-gain control

- To prevent excessive heat build-up in warmer seasons, we introduce two criteria for summer-mode activation:

  (i) Vertical Façade Irradiance ($E_f \geq 150\,\mathrm{W\,m^{-2}}$). When the solar irradiance striking the façade exceeds $150\,\mathrm{W\,m^{-2}}$, as the most typical threshold in dynamic shading control [25], there is a significant risk of solar heat gain through the glazing;

  (ii) 168-Hour (one week) Moving Average Air Temperature ($T_{rm} > 17\,°\mathrm{C}$): By calculating the average outdoor air temperature over the past seven days, the system ensures that shading for heat mitigation only takes place during genuinely warm periods, avoiding unnecessary closures during cooler transitional days.

- If and only if both conditions of $E_f \geq 150$ W/m² and $T_{rm} > 17$ °C are met, the external blind is lowered to 75% of full deployment (i.e., three-quarters closed). This intermediate height strikes a balance between reducing incident solar heat—lowering cooling loads—and preserving occupants' view and daylight access through the upper window segment.

By integrating these two control layers, the system remains sensitive to occupant comfort (through glare-avoidance) while limiting the overheating (through solar gain control) in desired climatic conditions. The general control scheme is represented in table 2.5 and table 2.6. The more detailed visualization of the control strategy is shown as a flowchart in Figure .

Table 2.5: Fabric roller blind - Glare-avoidance control

State	**Fabric height**	**DGP** threshold	**OR**	**DS–D** (sun in field-of-view)	E_f threshold
0	None	< 0.35	or	yes	$> 450\,\mathrm{W\,m^{-2}}$
1	¼ window	< 0.35	or	yes	$> 450\,\mathrm{W\,m^{-2}}$
2	½ window	< 0.35	or	yes	$> 450\,\mathrm{W\,m^{-2}}$
3	¾ window	< 0.35	or	yes	$> 450\,\mathrm{W\,m^{-2}}$

DS–D = direct sunlight on desk.
DGP = Daylight Glare Probability.
E_f = vertical Irradiance on the facade.

Table 2.6: Fabric roller blind - Solar-gain control

State	**Fabric height**	T_{rm} (°C)	E_f ($\mathrm{W\,m^{-2}}$)
0	None	-	-
1	¼ window	-	-
2	½ window	-	-
3	¾ window	> 17	> 150

T_{rm} = running mean outdoor temperature for one week.
E_f = solar irradiance on facade.

2.3.3 Electrochromic glazing – upper window: Glare-avoidance control and Solar-gain control

Glare-avoidance control

The electrochromic glazing adjusts its tint level based on the presence of direct sunlight detected by two types of sensors: vertical sensors positioned at eye level and horizontal sensors placed on the desk. If no direct sunlight is detected by any of the six sensors, the window remains in its clear state. However, if direct sunlight is visible at eye level, the glazing darkens to its maximum tint level, corresponding to 1% visible light transmittance. If sunlight is detected only by the horizontal desk sensors, the window transitions to a lighter tint (state 1), which allows approximately 40% of visible light to pass through. A detailed explanation of the tint states and their corresponding sensor conditions is provided in table 2.7 and table 2.8.

Solar-gain control

The control strategy follows the same logic as that used for external blinds but applies more precisely defined thresholds for tint transitions, as confirmed by the manufacturers. Specifically, two thresholds are defined for the running average of outdoor air temperature: 17 °C and 20 °C. In addition, three distinct thresholds are set for façade irradiance: $150\,\mathrm{W\,m^{-2}}$, $250\,\mathrm{W\,m^{-2}}$, and $450\,\mathrm{W\,m^{-2}}$. These thresholds determine the activation of different tint states based on environmental conditions. The general logic of how these thresholds are applied and how they influence the control signals are shown in table 2.7 and table 2.8. The more detailed visualization of the control strategy is shown as a flowchart in fig. 2.8.

2.3.4 Electrochromic glazing – lower window: Solar-gain control only

Glare-avoidance control is not applied to the lower electrochromic pane, as it is positioned below the 1.2 m eye level of a seated occupant and thus does not contribute significantly to glare. Instead, the lower pane operates solely based on solar-gain control. This control uses the similar environmental criteria with the upper pane, with threshold values of 17 °C and 20 °C for the running average outdoor temperature, and 150 W m^{-2}, 250 W m^{-2} for façade irradiance. The general logic for how these thresholds trigger different tint states is presented in table 2.8.The more detailed visualization of the control strategy is shown as a flowchart in fig. 2.8.

Table 2.7: Eelctrochromic glazing - Glare-avoidance control

Window segment	**DS-FOV[1]**	**DS-D[2]**	**EC level**
Upper	no	no	0
	no	yes	1
	yes	yes / no	3
Lower	no condition		0

[1] *DS-FOV*: direct sun in occupant's field of view.
[2] *DS-D*: direct sun on any desk sensor.

Table 2.8: Eelctrochromic glazing - Solar-gain control

Window segment	T_{rm} condition[3]	E_f condition[4]	**EC level**
Upper	$17 < T_{rm} < 20$ °C	$150 < E_f < 250$ W m^{-2}	1
	$17 < T_{rm} < 20$ °C	$250 < E_f < 450$ W m^{-2}	2
	$T_{rm} > 20$ °C	$E_f > 450$ W m^{-2}	3
Lower	$17 < T_{rm} < 20$ °C	$150 < E_f < 250$ W m^{-2}	1
	$T_{rm} > 20$ °C	$E_f > 250$ W m^{-2}	2

[3] T_{rm} =Running-mean outdoor temperature.
[4] E_f =Facade-normal solar irradiance.

2.4 Control schemes - outside usage hours

Summer mode

An additional control strategy is implemented during non-occupied hours—defined as weekdays from 6 p.m. to 8 a.m. and the entire weekend—to optimize solar heat gains or losses depending on the season.

- In summer-mode, when the running mean temperature (T_{rm}) exceeds 17 °C, the system aims to minimize unwanted heat accumulation. During these periods:

  (i) fabric roller blinds are fully lowered;

  (ii) the electrochromic glazing is set to its darkest state.

- This prevents interior overheating and reduces the absorption of heat by high-inertia building materials, ultimately lowering cooling demand.

Non-summer mode

- Conversely, during non-summer periods, the strategy promotes passive heat gains to support heating needs:

  (i) fabric roller blinds remain retracted;

  (ii) the electrochromic glazing stays in its clear state

- This control strategy allows maximum solar radiation into the space during non-usage hours as a useful heat gain.

In the flowcharts visulazied in fig. 2.7 and fig. 2.8, the glare-avoidance and solar-gain control strategies for both fabric roller blind and electrochromic glazing is represented.

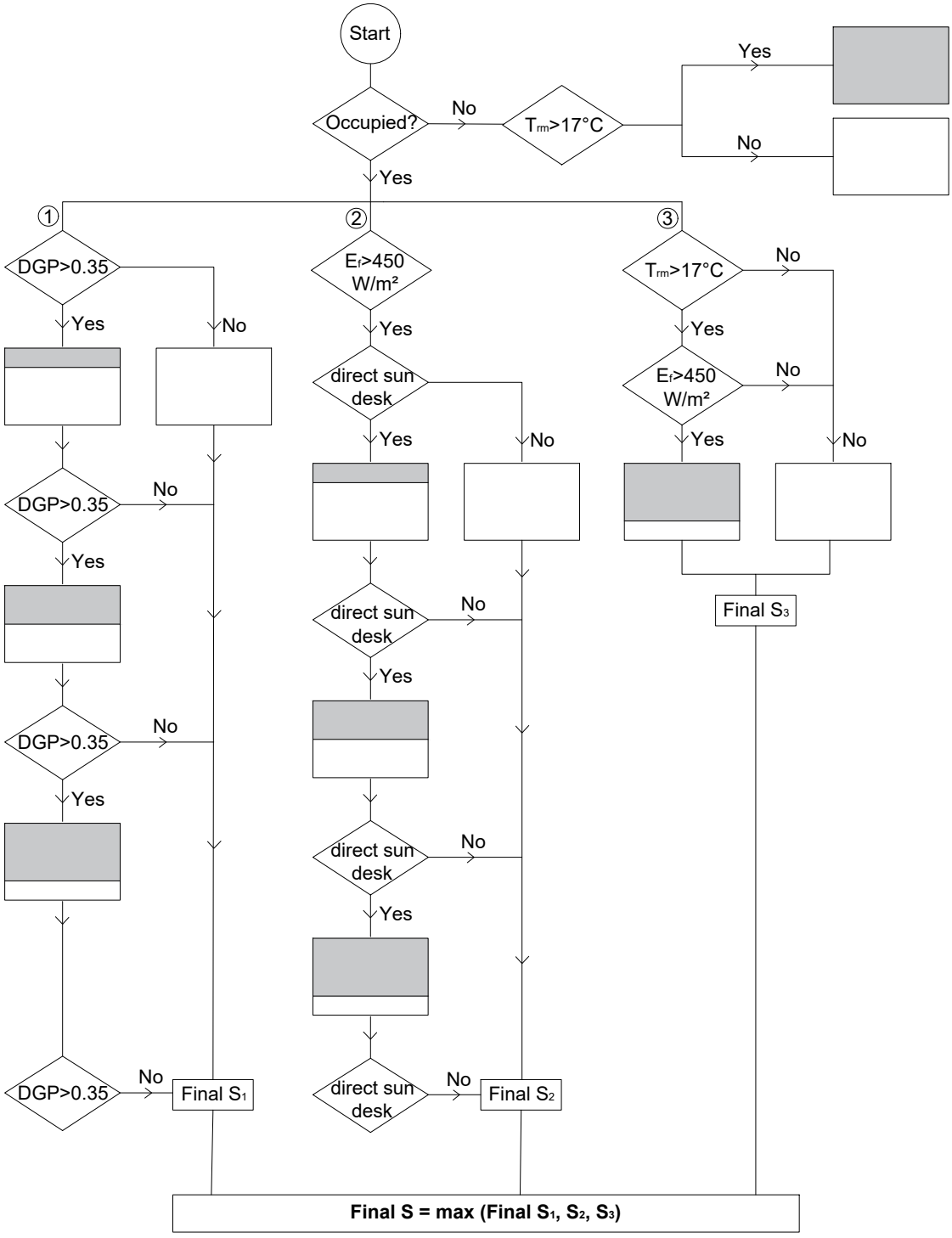

Figure 2.7: Control scheme - fabric roller blind

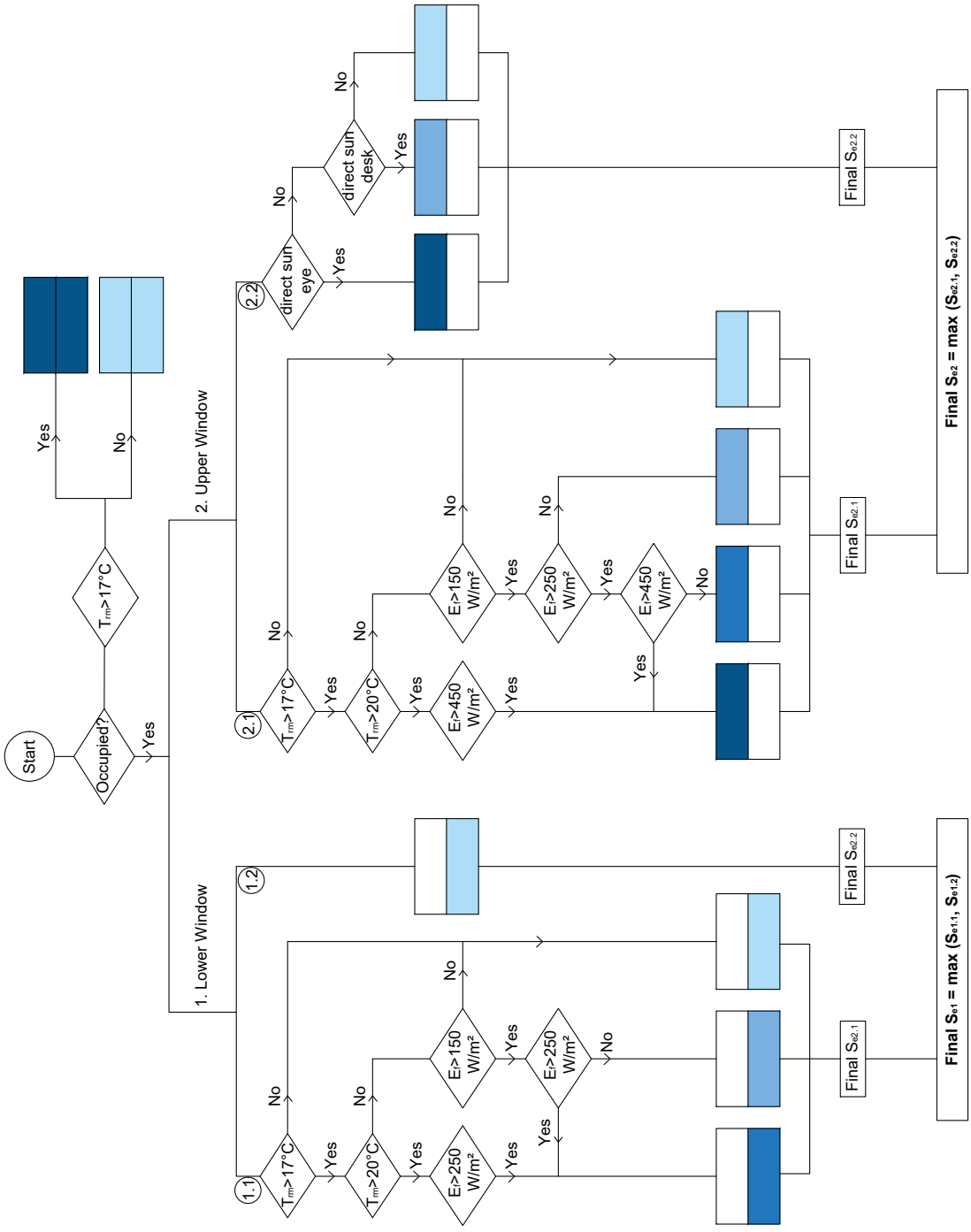

Figure 2.8: Control scheme - electrochromic glazing

2.5 Performance metrics and simulation tools

The performance analysis focuses on key metrics, including energy demand, as well as indoor daylight provision, glare perception, and daylight-induced non-visual potential. The following sections provide a detailed explanation of each performance metric, the corresponding evaluation indicators, and the simulation tools and setups used to conduct the analysis.

2.5.1 Energy demand

Annual heating, cooling and interior-lighting demands ($\mathrm{kW\,h\,m^{-2}}$) are used as the key performance indicators for energy demands because they normalize results to floor area, enabling a fair comparison between design. Hour-by-hour loads are simulated with the Honeybee + Ladybug tools [22] in Grasshopper, which automatically builds an EnergyPlus engine model from Rhino geometry and the weather data [26]. The following table detail the specific setup applied for evaluating energy demand, focusing exclusively on the components and configurations implemented in Grasshopper.

Table 2.9: Core modeling assumptions.

Input category	**Core assumption**
Occupancy	Weekdays 08:00–18:00 (reduced 12:00–13:00); density = $0.071\,\mathrm{pers\,m^{-2}}$ ($\approx 14\,\mathrm{m^2\,pers^{-1}}$).
Electrical equipment	Schedule mirrors occupancy; equipment power density = $11\,\mathrm{W\,m^{-2}}$.
Infiltration	$0.0013\,\mathrm{m^3\,s^{-1}\,m^{-2}}$ of exposed façade at 4 Pa.
Mechanical ventilation	Design flow = 1 ACH(air changes per hour), demand-controlled by occupancy.
Thermostat set-points	Heating 19.5 °C (setback 19 °C); cooling 24 °C.
Electric lighting	Installed LPD = $11\,\mathrm{W\,m^{-2}}$; annual dimming based on daylight simulation (500 lx target).
Heat recovery	Sensible heat-recovery unit with effectiveness factor 0.7.

2.5.2 Daylight provision

Spatial Daylight Autonomy (sDA) is used as the primary indicator to evaluate daylight provision. sDA is defined as the percentage of floor-area that receives at least 300 lux of daylight for at least 50 % of the annual occupied hours [24]. The following sections explain the simulation workflow to evaluate the spatial daylight autonomy:

Climate-based annual simulation

The study uses Honeybee + Ladybug Tools [22] inside the Grasshopper environment [21], which wrap the validated Radiance engine to run full-year (8760-hour) daylight calculations. A sensor grid covering the entire floor area (at the height of 750 mm from the floor which is equivalent to the working desk) records illuminance each hour, from which the sDA statistic is extracted.

Complex optics with BSDFs

Standard materials in Grasshopper libraries cannot capture the highly directional scattering of shading systems. Therefore, Bidirectional Scattering Distribution Function (BSDF) files are generated with genBSDF [27]. The BSDF describes, for every incident direction, how much light is transmitted or reflected into each outgoing direction, enabling accurate ray-tracing through complex assemblies [28]. Integrating these BSDFs into the Honeybee recipe allows the simulation to predict both diffuse sky contributions and sharp sun-patches after multiple bounces, giving a far more realistic estimate of sDA than simpler transmittance-only models.

2.5.3 Glare perception

Glare is formally defined by the International Commission on Illumination (CIE) as a "condition of vision in which there is discomfort or a reduction in the ability to see details or objects, caused by an unsuitable distribution or range of luminance, or by extreme contrasts." [29] . Since the space is lit primarily by daylight, the indicator to analyze glare percention is 95th percentile Daylight Glare Probability (DGP), introduced by Wienold and Christoffersen in 2006. Unlike older indices that look only at the brightest patch or the average luminance, DGP accounts for the combined effect of (i) the overall vertical eye illuminance and (ii) every bright element in the field of view—its luminance, size and position relative to the observer's line of sight [30]. The output is a single number between 0 and 1 that expresses a value that is not exceeded for more than 5 % of the occupied time, and it includes four different classes and relative DGP threshold as shown in table 2.10 [31].

Table 2.10: Daylight glare comfort classes and corresponding DGP thresholds

Daylight glare comfort class	**DGP threshold**
Imperceptible glare	$0.00 \leq \text{DGP} < 0.35$
Perceptible glare	$0.35 \leq \text{DGP} < 0.40$
Disturbing glare	$0.40 \leq \text{DGP} < 0.45$
Intolerable glare	$0.45 \leq \text{DGP} < 1.00$

DGP were computed with Raytraverse [32] , a Radiance-derived workflow purpose-built for view-dependent climate-based daylight simulations. Wasilewski et al. in 2022 validate its wavelet-guided adaptive-sampling engine against high-resolution rpict renders and show that it reproduces annual vertical eye illuminance and Daylight Glare Probability within ± 3 % while reducing computation time and storage by an order of magnitude. Because Honeybee and Ladybug focus on grid-based illuminance, their default recipes must re-render the scene for every camera position and tend to introduce sampling noise and glare-peak under-prediction when the view direction changes. Raytraverse, by contrast, stores the hemispherical light field once and can query any viewpoint or hour without rerunning the ray tracing, giving both higher accuracy and far greater efficiency for occupant-centred analyses. For these reasons, all view-dependent results reported in this study were generated with Raytraverse rather than the standard Honeybee and ladybug tools glare components.

2.5.4 Daylight non-visual potential

The daylight-driven non-visual potential of the space is quantified with melanopic equivalent daylight illuminance(mel-EDI). mel-EDI is defined as the illuminance of the CIE standard daylight spectrum D65 that would generate the same melanopic-weighted irradiance at the eye as the test light; in other words, it translates any spectrum into its "daylight-equivalent" circadian stimulus and is the reference metric named in both CIE S 26 2018 [33] and EN 17037 [24].

For the spectral handling in the model, all opaque room finishes and the fabric roller blinds are treated as spectrally neutral, so they preserve the spectral distribution of light. However, the six glazing variants (solar control, low-E, four electrochromic tint states) have wavelength-dependent transmittance and therefore alter the melanopic content of the daylight.

To evaluate mel-EDI, two main parameters are obtained:

- **Melanopic Daylight Efficacy Ratio (mel-DER)**: Defined as "the ratio of the melanopic efficacy of a test light source to the melanopic efficacy of the CIE standard illuminant D65 (reference daylight spectrum) at the same photopic illuminance" [24]. mel-DER for all glazings is obtained via a validated Excel tool by Hauser et al [34]. They developed and validated an Excel-based computation tool that characterizes both the colorimetric and photobiological performance of glazing systems. In this tool:

  (i) **Spectral inputs**: Users select a pre-transmittance spectral power distribution (SPD), such as CIE D65.

  (ii) **Glazing database**: The tool allows the creation of a library of glazing or optical materials, each defined by its spectral transmission curve (and bidirectional reflectance, if needed).

  (iii) **Layered Assembly**: Users assemble glazing units of one to three panes; the tool automatically computes the composite SPD after accounting for inter-pane reflections.

  (iv) **Output metrics**: From the transmitted SPD, the tool calculates: (1) Colorimetric indices (e.g., CRI, CIE TM-30 metrics adapted into the IES TM-30 framework), (2) Photobiological metrics, including mel-DER and melanopic equivalent daylight illuminance (mel-EDI), by applying the CIE S 026 melanopic action spectrum to the transmitted SPD.

  In this study, the SPD values are extracted from Optics [35] and after entering these data in the excel tool, the final mel-DER is extracted and represented in table 2.11 for all type of glazings.

- **Photopic Illuminance (E_p)**: This parameter was produced with Raytraverse as an hour-by-hour vertical eye illuminance at 1.20 m above the floor, using the same view-based ray-tracing set-up as the glare study.

Table 2.11: Melanopic Daylight Efficacy Ratio (Mel-DER) for Different Glazing Types

Glazing type	Solar control glazing	Low-E glazing	EC State 0	EC State 1	EC State 2	EC State 3
Mel-DER	1.02	1.00	0.90	0.96	1.36	1.52

As daylight entering the space is only altered through the glazing, the mel-EDI can be easily determined by modifying the photopic illuminance through the mel-DER:

$$\text{mel-EDI} = \text{mel-DER} * E_{\text{p}} \tag{2.1}$$

finally, to express daylight's non-visual potential over the year, a new metric is developed as melanopic daylight autonomy, **mel-DA**: the percentage of occupied daytime hours during which mel-EDI at the eye is $\geq$ 250 lux. The 250 lux benchmark is the daytime minimum recommended by Brown et al. for supporting alertness, mood, and circadian entrainment [36].

The 250 lux melanopic EDI threshold recommended by Brown et al. is not an arbitrary value, but the product of an expert-consensus process grounded in both laboratory and real-world evidence. Here's what it means and hOW it was chosen:

- **Defintion and measurement**: Melanopic Equivalent Daylight Illuminance (melanopic EDI) quantifies light's ability to stimulate the intrinsically photosensitive retinal ganglion cells (ipRGCs)—the cells most responsible for non-visual effects such as alertness and circadian entrainment. Vertical illuminance at eye level (approximately 1.2 m height, seated), using a spectroradiometer or calibrated sensor to weight light according to the melanopic action spectrum .

- **Consensus Process**: Brown and colleagues convened a multi-day workshop of circadian-light experts, systematically reviewing laboratory studies on melatonin suppression, circadian phase-shifting, and subjective alertness, then voting to reach agreement on practical lighting targets for healthy adults aged 18–55.

- **Physiological Rationale**: Controlled studies show that non-visual responses (melatonin suppression, phase shifts, alerting effects) rise sigmoidally with melanopic EDI, spanning roughly 1–1 000 lux (civil twilight to bright daylight). The mid-range, around 250 lux, corresponds to the steepest part of these response curves—where additional increases in light yield substantial gains in physiological activation. Moreover, alertness and mood: A meta-analysis found that "bright" conditions (>500 lux photopic, equivalent to >250 lux melanopic EDI using conservative conversion factors) produced significant alerting effects in 80 % of studies, compared to "dim" (<80 lux photopic) conditions.

- **Real-World Evidence**: In office workers, boosting daytime lighting from typical fluorescent setups (<150 lx melanopic EDI) up to 250–290 lx led to measurable improvements in sleep quality, mood (reduced depression and anxiety), and cognitive performance. Also, energy implications: Achieving 250 lx melanopic EDI in a standard open-plan office may require roughly a 50 % increase in horizontal illuminance (e.g., from 300–400 lux to 600 lux) or use of daylight and higher-DER (melanopic daylight efficacy ratio) luminaires.

By separating the spectral term (mel-DER) from the photopic illuminance (E_p), this workflow remains computationally light abd flexible, delivering a robust, occupant-centred assessment of daylight's biologically effective power.

Chapter 3

Results

3.1 Activation frequency

Table 3.1 shows in percentage how often each shading system enters its various deployment states across different climatic zones, based on different factors which is discussed in chapter 2. Moreover, in figs. 3.1 to 3.3, the activation frequency for each shading system in each climate is visualizied for a better hour-and-state understading. In all climates studied, the intermediate positions—where fabric covers half or three-quarters of the window height—are engaged quite frequently. These partial deployments strike a balance between glare control and daylight admission, offering improved outward visibility compared to a fully lowered shade; however, even at half or three-quarters height, fine details outside the building may appear muted or slightly obscured. Additionally, the elecetrochromic darkest state is also occured regularly. While this mode provides maximal protection against solar heat gain, its high level of tint can significantly diminish the clarity of the view and cause a color shift in the view as well due to its blue tinting.

Table 3.1: Activation frequency of control strategies during usage hours for different locations

State	Frankfurt			Stockholm			Rome		
	sc+ib[1] [%]	lowE+eb[2] [%]	EC[3][%]	sc+ib [%]	lowE+eb [%]	EC [%]	sc+ib [%]	lowE+eb [%]	EC [%]
0	23	34	36	35	30	34	36	15	42
1	12	19	25	13	8	26	19	13	20
2	36	31	2	34	41	4	22	28	2
3	29	16	37	18	21	36	23	42	36

[1] *sc+ib*: Solar control glazing + Internal fabric roller blind
[2] *lowE+eb*: Low-E glazing + External fabric roller blind
[3] *EC*: Electrochromic glazing. Only upper-window activation is shown.
Note: Activation frequency during usage hours only is presented.

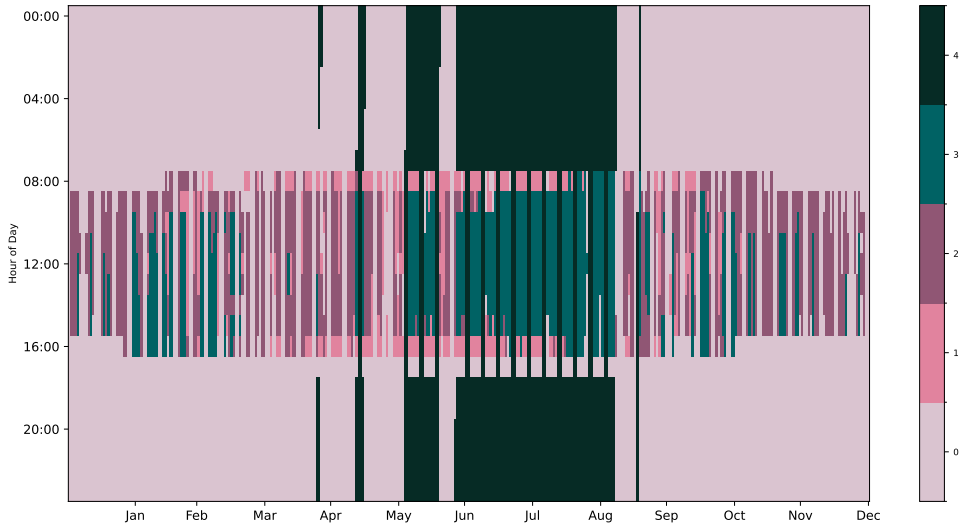

(a) lowE glazing + External fabric roller blind (b3).

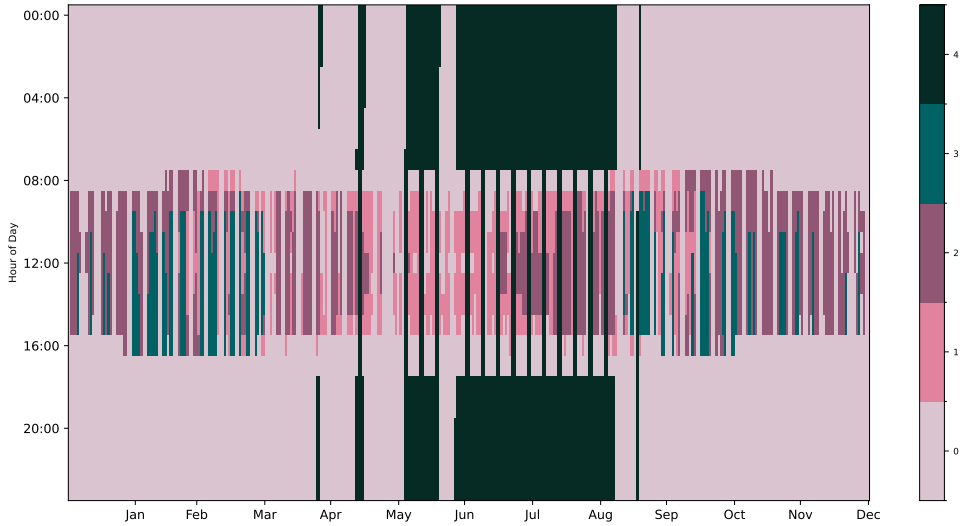

(b) Solar cotrol glazing + Internal fabric roller blind (b3).

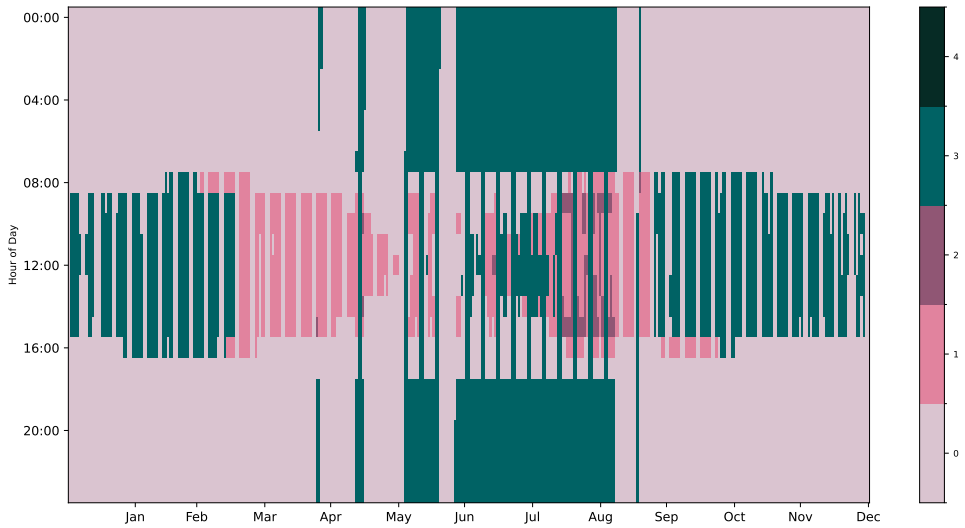

(c) Electrochtromic glazing - upper window.

Figure 3.1: Activation frequency of shadings - Franfurt. Fabric: 0: No shading, 1: 1/4 of height, 2: 2/4 of height, 3: 3/4 of height, 4: full height. Electrochromic glazing: 0: 65% transmittance, 1: 40% transmittance, 2: 6% transmittance, 3: 1% transmittance, 4:-.

(a) lowE glazing + External fabric roller blind (b3).

(b) Solar cotrol glazing + Internal fabric roller blind (b3).

(c) Electrochtromic glazing - upper window.

Figure 3.2: Activation frequency of shadings - Stockholm. Fabric: 0: No shading, 1: 1/4 of height, 2: 2/4 of height, 3: 3/4 of height, 4: full height. Electrochromic glazing: 0: 65% transmittance, 1: 40% transmittance, 2: 6% transmittance, 3: 1% transmittance, 4:-.

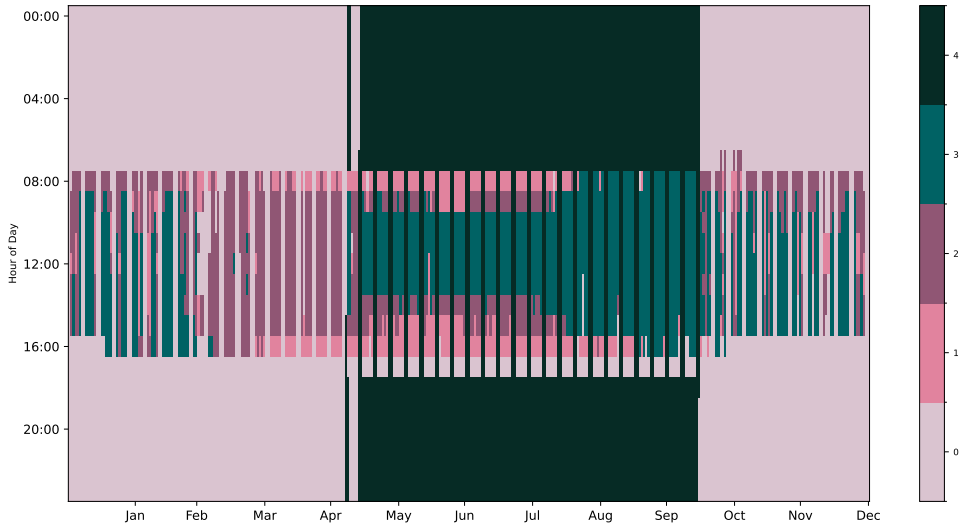

(a) lowE glazing + External fabric roller blind (b3).

(b) Solar cotrol glazing + Internal fabric roller blind (b3).

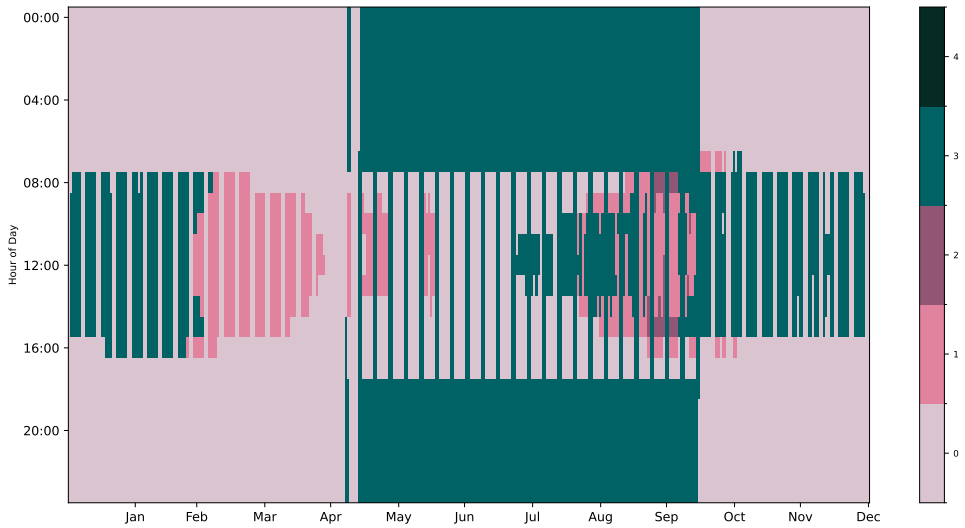

(c) Electrochtromic glazing - upper window.

Figure 3.3: Activation frequency of shadings - Rome. Fabric: 0: No shading, 1: 1/4 of height, 2: 2/4 of height, 3: 3/4 of height, 4: full height. Electrochromic glazing: 0: 65% transmittance, 1: 40% transmittance, 2: 6% transmittance, 3: 1% transmittance, 4:-.

3.2 Performance results - Eenrgy demand

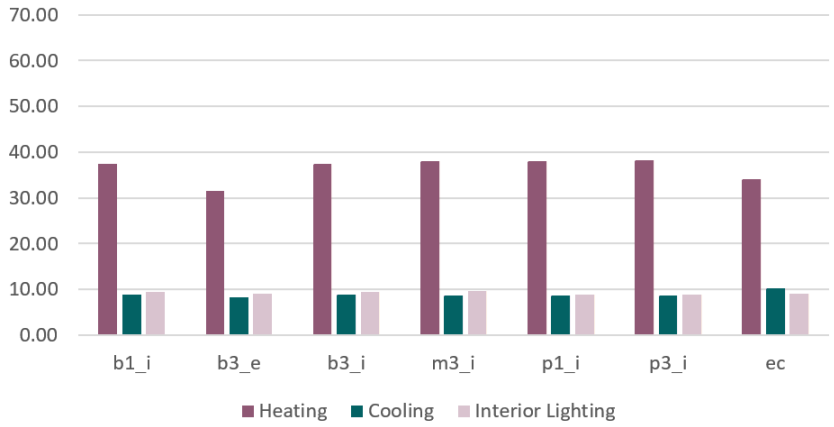

(a) Frankfurt

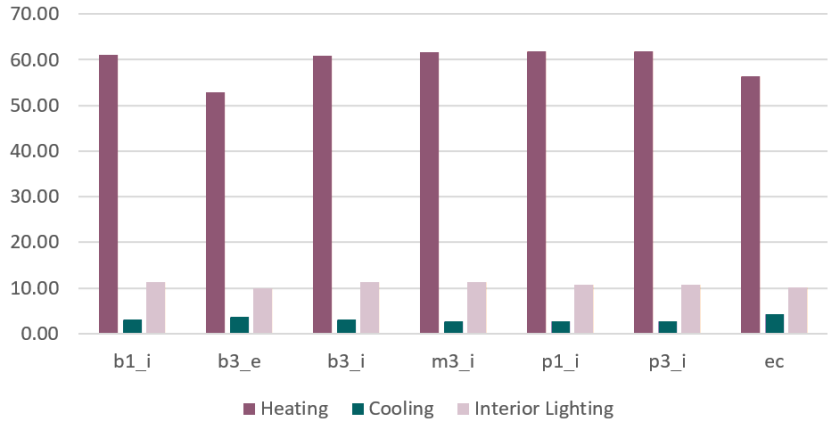

(b) Stockholm

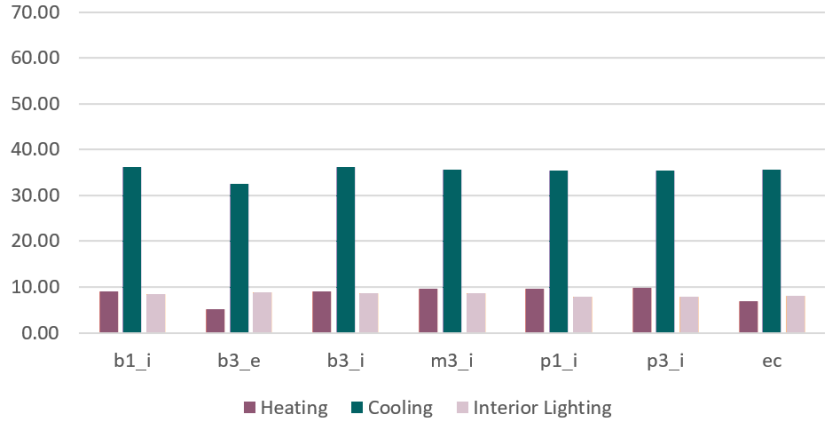

(c) Rome

Figure 3.4: Energy demand results. Configuration naming: b(black), p(pearl), m(metalized), ec(electrochromic) , 1(openness factor:1%) , 3(openness:3%), i(interior), e(exterior)

According to fig. 3.4, across all climates, the total annual (heating + cooling + lighting) difference between the lowest- and highest-energy configuration is under 10 kWh/m² · yr—typically a 10–15 % swing on a baseline of 50–70 kWh. In practical terms, all seven configurations perform within a relatively narrow band. In the following sections a more detailed analysis of the results for heating, cooling, and interior lighting is provided.

3.2.1 Heating demand

Interior-blind variants—whether black, pearl, or metalized and at 1 % or 3 % openness—produce virtually identical annual heating loads in all three cities. In Rome, these configurations require approximately 9–10 kWh/m² · yr; in Frankfurt, about 37–38 kWh/m² · yr; and in Stockholm, roughly 61–62 kWh/m² · yr. By contrast, relocating the same black blind (3 % openness) to the exterior of the glazing and changing the glazing itself to a low-emissivity (low-E) type significantly reduces heating demand. Compared to any interior-blind arrangement, this combination cuts heating requirements by about 45 % in Rome, 16 % in Frankfurt, and 13 % in Stockholm. Furthermore, substituting static interior blinds with electrochromic glazing yields an even greater reduction in heating load—on the order of 20 % in Rome and approximately 10 % in both Frankfurt and Stockholm.

3.2.2 Cooling demand

In Rome, both interior blinds and electrochromic (EC) glazing yield an annual cooling demand of approximately 36 kWh/m² · yr. Installing a black exterior blind with 3 % openness instead of the the same interior blind reduces that requirement to about 32 kWh/m² · yr, representing roughly an 11 % saving. In Frankfurt, interior blinds incur around 9 kWh/m² · yr of cooling load, while the exterior black blind lowers this slightly to about 8 kWh/m² · yr—again an approximate 11 % reduction. Interestingly, electrochromic glazing increases the cooling demand to around 10 kWh/m² · yr, which is between 11 % and 25 % higher than the figure for an interior blind. In Stockholm, cooling loads are minimal, ranging from about 2.5 to 4 kWh/m² · yr. An exterior blind actually raises the annual cooling demand by 20 % to 50 %; by comparison, interior blinds maintain loads of roughly 2.5 to 3.0 kWh/m² · yr, and EC glazing uses about 4.3 kWh/m² · yr.

3.2.3 Interior lighting demand

In general, the difference in interior lighting demand between different shading systems is not signigficant. In detail, black and metalized interior blinds (b1_i, b3_i, m3_i) incur the highest lighting load, ≈ 8.5 kW h to 11 kW h across the three climates. Pearl (white) interior with 3 % openness (`p3_i`) or EC glazing consistently reduce lighting by 4 % to 11 % relative to dark fabrics (e.g. 8.1 kW h vs. 9 kW h in Rome; 8.5 kW h vs. 9.5 kW h in Frankfurt; 10 kW h vs. 11 kW h in Stockholm). Exterior black blinds cost ≈ 9 kW h in Rome/Frankfurt and ≈ 10 kW h in Stockholm—comparable to black interiors and 5 % to 10 % worse than pearl or EC.

The key takeaways for design decisions based on only energy demand could be:

- Placing a black fabric blind outside (3 % open) consistently reduces both heating and cooling (up to 45 % and 10 % respectively).

- If exterior shading is not possible, electrochromic glazing yields roughly 10–20 % lower heating than a static interior blind, but requires more cooling.
- Among interior blinds, color (black vs. pearl vs. metalized) and small openness changes (1 % vs. 3 %) do not affect heating or cooling; they only shift lighting by about 0.5–1 kWh.

By quantifying each configuration's 10–50 % shift in heating/cooling or its 4–11 % shift in lighting—and noting that the absolute energy difference remains under 10 kWh/m² · yr—you can see that all variants perform fairly similarly. This suggests that other factors are more effective in the performance of the shading systems, and through the whole path of this project, it is concluded that the control strategy itself is more effective which will be explained later in chapter 4.

3.3 Performance results - Daylight provision

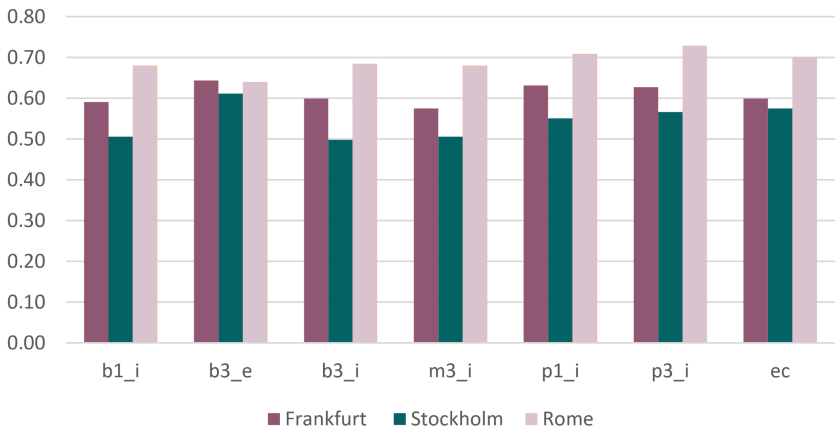

Figure 3.5: sDA results (Spatial Daylight Autonomy). Configuration naming: b(black), p(pearl), m(metalized), ec(electrochromic) , 1(openness factor:1%) , 3(openness:3%), i(interior), e(exterior)

The spatial daylight autonomy (sDA) results in fig. 3.5 reveal only modest variation across the seven shading configurations—b1_i, b3_e, b3_i, m3_i, p1_i, p3_i, and EC glazing—when assessed in Frankfurt, Stockholm, and Rome.

In Frankfurt, the exterior black fabric blind with 3 % openness (b3_e) achieves sDA=0.64 (64 %), about a five–percentage–point gain over the lowest interior–blind result, m3_i (sDA=0.57). Pearl interiors and EC glazing also score highly: p1_i (1 % openness) reaches sDA=0.63, while p3_i and EC glazing each hover near 0.60 to 0.62. Black interior fabrics (b1_i, b3_i) lie in the 0.59 to 0.60 range. Altogether, all seven configurations in Frankfurt fall within a narrow band of 0.57 to 0.64.

In Stockholm, daylight is more limited, yet the same exterior black blind leads with sDA=0.61—eleven percentage points above the lowest interior result (b3_i and m3_i, each at sDA=0.50). EC glazing and p3_i each score about 0.57, roughly six points above the darkest interiors (0.50–0.51). The pearl interior at 1 % openness (p1_i) yields sDA=0.55. Despite b3_e's advantage, the full range of sDA across all configurations remains under 0.11, clustered between 0.50 and 0.61.

In Rome, the ranking shifts: p3_i (pearl, 3 % openness) tops the list with sDA≈0.73, whereas b3_e falls to about 0.64, nine points lower. EC glazing and p1_i both achieve sDA≈0.70, three points below p3_i and six points above b3_e. Dark or metalized interiors (b1_i, b3_i, m3_i) cluster near sDA=0.68. Although differences appear larger under bright Mediterranean skies, the overall spread is still under ten points (0.64–0.73), so even the lowest option meets the sDA threshold in most hours of the year.

Across the three climates, two trends emerge:

- Exterior black blinds boost sDA by 4 % to 11 % in cooler climates (Frankfurt, Stockholm) by admitting more diffuse light, whereas in Rome they reduce sDA by about 9 % compared to light-colored interiors due to the higher frequency of shading activation during summer.
- EC glazing consistently delivers sDA in the 0.57 to 0.70 range—within 2 % to 7 % of the best static option in each climate, and improving over dark interior fabrics by a similar margin.

These limited variations suggest that with a logical dynamic control algorithm and considering energy-use trade-offs,sDA remains above minimum thresholds.

3.4 Performance results - Glare perception

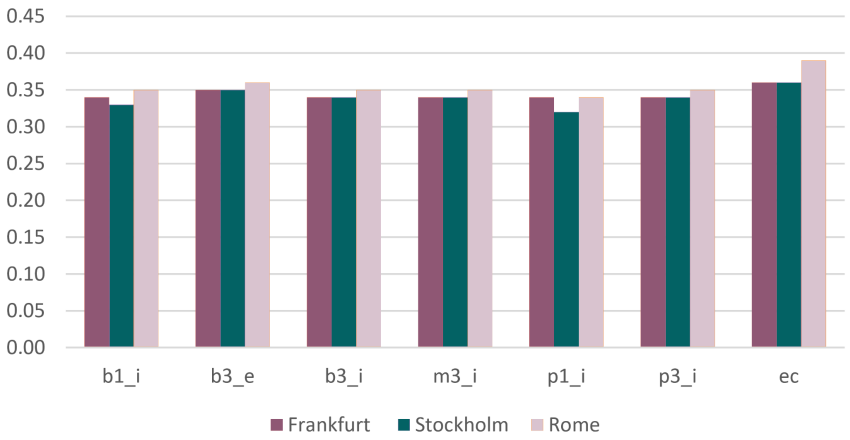

Figure 3.6: DGP results (Daylight Glare Probability). Configuration naming: b(black), p(pearl), m(metalized), ec(electrochromic) , 1(openness factor:1%) , 3(openness:3%), i(interior), e(exterior)

The annual 95th-percentile DGP (Daylight Glare Probability) values show only minor variation among the six fabric-blind configurations—b1_i, b3_e, b3_i, m3_i, p1_i, p3_i—within each climate, while electrochromic glazing (ec) raises DGP enough to exceed the EN 17037 glare classification by one class (refer to table 2.10).

In Frankfurt, all fabric blinds yield a 95th-percentile DGP in the narrow range of 0.33 to 0.35. The exterior black blind at 3 % openness (b3_e) sits near the upper end (≈ 0.35). With electrochromic glazing, the 95th-percentile DGP rises to ≈ 0.36—0.01 to 0.03 higher than any fabric blind—shifting from imperceptible glare to perceptible glare

(table 2.10). Although the absolute increase is small, it indicates that in Frankfurt's office, electrochromic glazing permits marginally more peak-day glare potential than a fabric blind, despite benefits such as higher sDA and lower heating loads.

In Stockholm, daylight levels are lower, yet the six fabric blinds again cluster tightly with 95th-percentile DGPs spanning 0.32 to 0.35. Black interior at 1 % openness (b1_i) is ≈ 0.33; black interior at 3 % or metalized interior (b3_i, m3_i) ≈ 0.34; exterior black blind (b3_e) ≈ 0.35; pearl fabrics (p1_i, p3_i) ≈ 0.34–0.35. All fall in the EN 17037 "Imperceptible glare" class. With electrochromic glazing, the 95th-percentile DGP increases to ≈ 0.36–0.37—0.02 to 0.04 above fabric blinds—shifting classification in the same way As in Frankfurt, this modest jump reflects a slight increase in direct luminance at the brightest hours, moving the glare risk one level higher under EN 17037 thresholds.

In Rome's bright Mediterranean climate, the six fabric-blind options again yield similar DGPs—≈ 0.34–0.35. Pearl interiors (p1_i, p3_i) produce ≈ 0.34; black interiors (b1_i, b3_i) and metalized (m3_i) ≈ 0.35; exterior black blind (b3_e) ≈ 0.35. By contrast, elecetrochromic glazing raises the 95th-percentile DGP to ≈ 0.39—a 0.04 to 0.05 increase over fabric blinds, which is the same in Frankfurt and Stockholm.

Across all three climates:

- The six fabric-blind configurations show remarkably consistent DGP values—spanning at most 0.03 units—underscoring that color, material (fabric vs. metalized), openness (1 % vs. 3 %), and mounting (interior vs. exterior) have negligible effect on annual worst-case glare probability.

- The one notable outlier is elecetrochromic glazing, which consistently increases DGP by 0.01–0.05 over its fabric counterparts. This small rise is sufficient to move the glare classification for one class.

- Although this shift is modest in absolute terms, it is important: when elecetrochromic glazing is used to balance daylight autonomy and solar control, designers must recognize that its highest tint state still admits more intense directional luminance than any closed fabric blind.

- Nevertheless, because all worst-case DGP values for fabric blinds already lie below or at the 0.35 threshold and EC glazing simply exceeds the threshold by 0.01 in Frankfurt and Stockholm, the practical difference in occupant discomfort is likely minor, except in Rome that this difference is by 0.04. As a result, once a baseline level of glare control is ensured, shading decisions may justifiably prioritize secondary factors—such as energy savings, occupant views, and overall daylight distribution—over small differences in annual DGP.

3.5 Performance results - Daylight non-visual potential

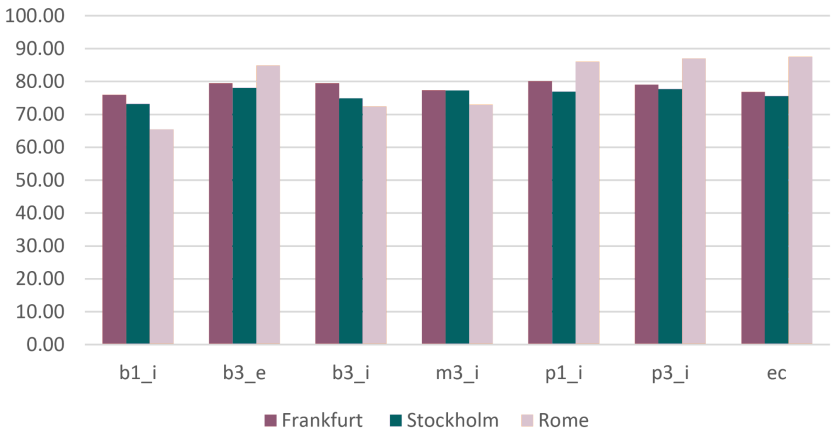

Figure 3.7: mel-DA results (Melanopic Daylight Autonomy). Configuration naming: b(black), p(pearl), m(metalized), ec(electrochromic) , 1(openness factor:1%) , 3(openness:3%), i(interior), e(exterior)

The melanopic daylight autonomy (mel-DA) results—defined here as the percentage of occupied hours during which melanopic equivalent daylight illuminance (mel-EDI) exceeds 250 lux—show consistently high values ($> 70\,\%$) in Stockholm and Frankfurt, whereas in Rome the choice of shading has a much larger impact.

In Frankfurt, all seven configurations (b1_i, b3_e, b3_i, m3_i, p1_i, p3_i, ec) yield mel-DA in the narrow range of approximately 76 %–80 %. Electrochromic glazing and black interior blinds at 1 % openness each reach around 76 %, while metalized interior at 3 % performs slightly better at 77 %. Black and pearl interior blinds at 3 % and exterior black at 3 % cluster near 79 %, with pearl interior at 1 % peaking at 80 %. In other words, any type of fabric and elecetrochromic glazing in Frankfurt provides mel-EDI > 250 lux for at least three-quarters of occupied hours.

In Stockholm, where daylight is intrinsically lower, the same seven strategies still yield mel-DA between about 73 % and 78 %. TThe lowest value, around 73 %, is for the black interior blind at 1 % openness. Black interior at 3 % and metalized interior reach about 75 %, electrochromic glazing follows at 76 %, and pearl interior at 1 % is near 77 %. The highest values, around 78 %, are achieved by exterior black at 3 % and pearl at 3 %. Once again, the total spread is only 5 percentage points, indicating that in Stockholm's overcast/diffuse-dominant sky, any shading choice still permits more than 70 % of hours above the 250 lux melanopic threshold.

In Rome's bright Mediterranean climate, mel-DA values range much more widely—from roughly 65 % up to 88 %—demonstrating how shading can significantly influence non-visual daylight potential when sunlight is abundant. A black interior blind at 1 % openness (b1_i) yields the lowest mel-DA at approximately 65 %, reflecting that its color and openness factor can effect blocking large portions of melanopic irradiance. Black interior at 3 % openness (b3_i) and metalized interior (m3_i) each reach about 73 %, whereas exterior black at 3 % openness (b3_e) jumps to roughly 85 %—a 12-point increase compared to b3_i. Pearl fabrics perform even better: pearl interior at 1 % (p1_i) yields about 86 %,

and pearl interior at 3 % (p3_i) about 87 %, each just 1–2 points above b3_e. The highest mel-DA is seen with electrochromic glazing (ec) at approximately 88 %, about 23 points higher than a low-openness black interior. Thus, in Rome, EC glazing and pearl fabrics maximize circadian-relevant daylight, while dark interior blinds reduce it.

Across the three climates:

- In Stockholm and Frankfurt, all seven shading configurations exceed 70 % mel-DA, and the spread remains under 5 percentage points, indicating that any fabric shade or elecetrochromic glazing provides sufficient non-visual daylight in cooler, lower-sun climates. In these contexts, designers can select shading based on energy or glare criteria without significant circadian-daylight penalty.
- In Rome, mel-DA spans 65 %–88 %, with pearl fabrics ($\approx$ 86–87 %) and elecetrochromic glazing ($\approx$ 88 %) outperforming exterior black ($\approx$ 85 %) by 1–3 points, and outperforming dark interiors by 12–23 points. Consequently, in a sun-dominant environment, selecting a light-colored interior blind or elecetrochromic glazing becomes critical for maintaining high levels of non-visual daylight.

Chapter 4

Discussion

The results in this study show that the absolute performance gap between any of the seven shading options is small. However, placing the device on the façade exterior consistently yields the most balanced outcome: in Frankfurt and Stockholm it trims heating demand by 13–16% and cooling by approximately 11% relative to an equivalent interior black fabric, while in Rome the combination of exterior placement and low-E glazing cuts the already-modest heating load by up to 45% and cooling by approximately 11%. By intercepting solar radiation before it reaches the cavity, the exterior blind prevents both winter conductive losses (thanks to the upgraded low-E pane) and summer solar gains. Electrochromic glazing slots into a clear middle ground. It lowers heating by 10–20 % compared with a static interior blind, yet still demands 10–50 % more cooling than the exterior fabric solution, illustrating that the insulating–radiative benefits of position outweigh the dynamic optical modulation of the pane itself.

Daylight-related metrics reinforce this hierarchy: in diffuse-dominant climates (Frankfurt, Stockholm) the exterior blind increases spatial daylight autonomy (sDA) by 4–11 percentage points over dark interior fabrics because it blocks glare outside while admitting more diffuse sky-light; in sun-rich Rome the same exterior device sacrifices ≈ 9 percentage points of sDA relative to a light-coloured interior blind because it shades too aggressively during peak hours. Electrochromic glazing again sits between the two, typically within ± 3 points of the best static option. However, the glare percetion is higher for electrochromic glazing than the fabric blind shading confinfigurations, always exceeding the 0.35 threshold, and finally for daylight non-visual potential, all the seven configurations are staistfying almost two-third of hours, except in Rome which shows some considerable variations between the shading systems and configurations.

Taken together, these patterns demonstrate that the mounting position of the shading layer is a stronger determinant of both energy and daylight performance than either fabric color/openness. Moreover, electrochromic glazing showed a better energy performance than internal blinds, aand similarlu in the study by Alkhatib et al. [11] reported electrochromic glazing outperforming “in-between-glass” roller blinds. This study shows also another important aspect significantly influential in the performance, which is the control strategy which will be explained in the next section.

4.1 Improtance of control strategy

The simulation process consistently showed that when and how the device responds is more influential than what the device is. This finding echoes Alkhatib et al. [11], who likewise concluded that algorithm design can outweigh the shading choice. The thresholds, control algorithms, and activation signals chosen for a dynamic shading system decisively shape its overall performance. If the control strategy is too simplistic or poorly calibrated, it can produce undesirable trade-offs—such as high daylight glare probability (DGP) alongside high spatial Daylight Autonomy (sDA); or, conversely, low glare coupled with inadequate daylight, excessive electric-lighting energy use, or insufficient melanopic equivalent daylight illuminance (mel-EDI). A carefully structured, well-tuned control logic is therefore essential to unlock the full potential of modern shading technologies.

4.1.1 Glare-avoidance control

The first iteration borrowed the World Meteorological Organization's "sunshine-hour" criterion (direct normal irradiance $\geq 120\,\mathrm{W\,m^{-2}}$) to trigger shading [37]. In practice that proxy proved too high: even a $40\,\mathrm{W\,m^{-2}}$ direct component could still drive annual 95th-percentile DGP values to ≈ 0.60—well into EN 17037's intolerable glare class.

Re-coding the algorithm to actuate on the predicted hourly DGP (target ≤ 0.35) instead of a fixed irradiance threshold aligned the model with observed occupant behavior: blinds deployed only when discomfort was likely, reducing hours of excessive luminance contrast.

4.1.2 Solar-gain control

Solar-gain control proved highly dependent on shading position (external/internal): when the "close the shade to 3/4 of height whenever the Running average outdoor temperature is more than 17 °C and the façade irradiance $(E)_f$ exceeds 150 $\mathrm{W\,m^{-2}}$" rule was applied to an interior blind, the fabric absorbed solar heat and re-radiated it indoors, so Frankfurt's cooling demand actually rose from 15.5 $\mathrm{kWh\,m^{-2}}$ (with no solar-gain control) to 17.5 $\mathrm{kWh\,m^{-2}}$ and spatial daylight autonomy decreased considerably; similar trends appeared in the other climates. The identical rule on an exterior blind, however, shed the absorbed energy to the outside and halved Frankfurt's cooling load to 7.5 $\mathrm{kWh\,m^{-2}}$. The contrast underlines that such marginal energy effects for internal blinds do not justify the accompanying compromise on daylight performance, particularly because the glazing itself already provides solar-control properties.

Regarding the specification of the thresholds for shading activation and their sensitivity, doubling E_f, for instance, from 150 to 300 $\mathrm{W\,m^{-2}}$ changed cooling by only about 1 $\mathrm{kWh\,m^{-2}}$ in Frankfurt, with similar effects in other climates. Therefore, the 150 $\mathrm{W\,m^{-2}}$ threshold was considered as the typical threshold for solar-gain control in shading systems [25].

4.2 Limitations and future development

This study's findings should be interpreted in light of some scope limitations that point directly to future research needs. One limitation is that all simulations used a single-person cellular office; applying the same façade options to an open-plan floor—where desks are set deeper in the space and neighboring workstations interact optically—could alter both daylight metrics and the practical feasibility of frequent shade movements.

Moreover, while exterior blinds consistently delivered the best energy balance, their real-world performance depends on local wind pressures that were not considered in the analysis; strong gusts can force the blinds to retract, potentially raising cooling loads in Rome or allowing direct-sun glare in Stockholm and Frankfurt. Integrating wind-speed data and control interlocks into the simulation loop would provide a more realistic estimate of these risk periods. In fig. 4.1, the wind speeds are provided.

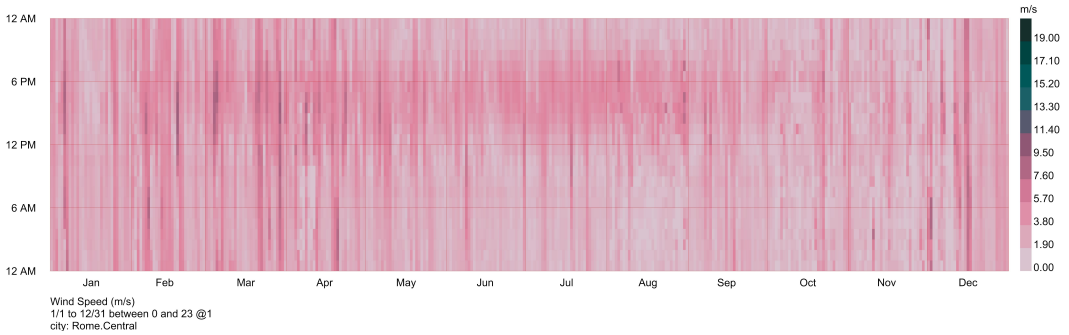

(a) Rome (Southern Europe).

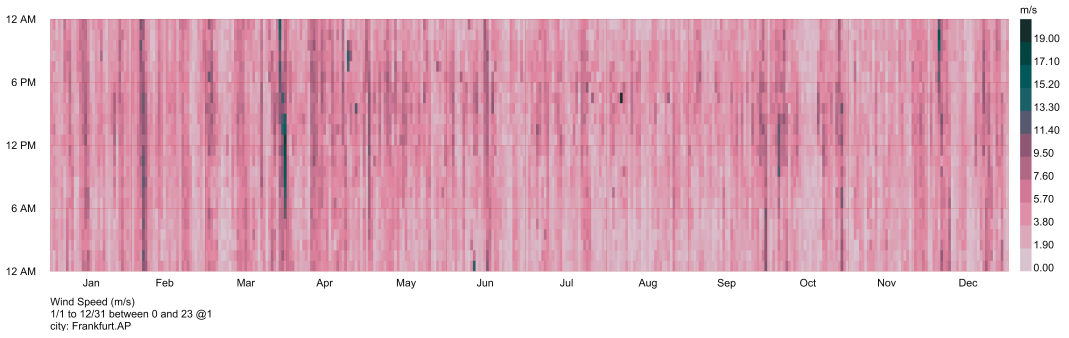

(b) Frankfurt (Central Europe).

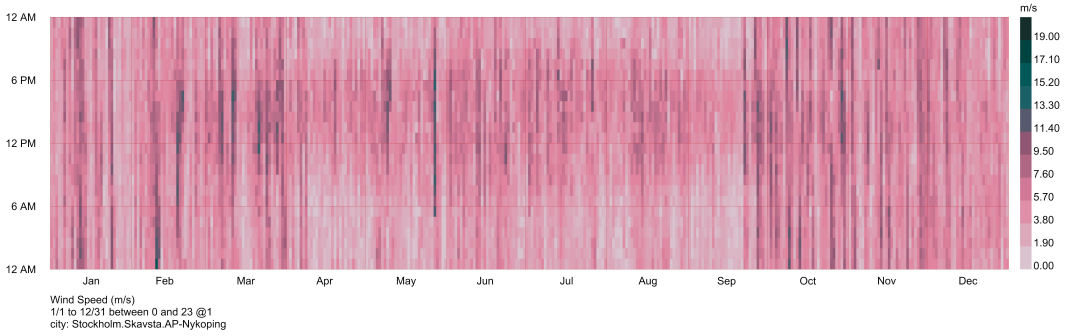

(c) Stockholm (Northern Europe).

Figure 4.1: Annual wind speed data in m/s for the three climates.

- Rome shows a 4-6 m/s band from April to September between roughly 14 h and 20 h – the same summer-afternoon window when solar gains and cooling loads peak. A wind with a speed near 6-8 m/s will often push the blinds to their cut-out point, so the energy-savings predicted for the south façade in the model are likely optimistic during those hot months.
- Stockholm has briefer but more frequent gusty episodes, mainly in the frontal passages of late winter/early spring and again in October–November. These bursts coincide with low-sun hours (09 h–15 h), so involuntary retraction could re-introduce direct-sun glare precisely when daylight is scarce.

- for Frankfurt, the graph reveals isolated wind hours—especially in mid-January, mid-March and October—where speeds spike well above 15 m/s. Although the cooling-load penalty is small at those times, glare control would still be lost.

Another limitation to consider is excluding the Venetian blinds in the study, whose adjustable slats can simultaneously redirect daylight and block direct sun; their angular selectivity might outperform the fixed-weave fabrics analyzed, particularly on east or west façades, and therefore merit a dedicated parametric study.

Although view quality is a critical comfort factor, comparison of view clarity across different system is not feasible! Because for fabric, the partial occlusion of fabrics and the unsharp view which happens due to refraction depends on openness factor and weaving of the fabric, and this refraction cannot be modelled accurately. For electrochromic glazing, there is the color shift which affect the view clarity. Also, if the tinting level between the two separate window panes are largely different, there is the problem of the adaptation level between different tints. There is no validated metric available to this date for view clarity to consider all these aspects for the comparison, that's why this is not included in the main analysis.

The control algorithms were evaluated purely on physical outputs (energy, glare, illuminance) without soliciting occupant feedback; incorporating user-centered studies could reveal whether the theoretically optimal strategies align with real preferences and acceptance.

Addressing these five gaps—spatial layout, wind interaction, Venetian-blind dynamics, view-quality metrics, and user behavior—will sharpen the predictive power of future façade studies and help translate simulation gains into reliable building practice.

Chapter 5

Conclusion

This study evaluated seven dynamic façade variants—electrochromic glazing, external fabric roller blind + lowE glazing and internal fabric roller blinds + solar control glazing—under an automated control framework with manual override. Their performance was analyzed and compared for a south-facing office in Stockholm (Northern Europe), Frankfurt (Central Europe), and Rome (Southern Europe) using four complementary criteria: annual energy demand (heating + cooling + lighting), spatial daylight autonomy (sDA), annual 95$^{\text{th}}$-percentile Daylight Glare Probability (DGP), and melanopic daylight autonomy (mel-DA).

5.1 Main findings

Across the three representative European climates analysed, all seven façade variants occupied a surprisingly tight energy band: the annual sum of heating, cooling, and lighting never differed by more than 10 kWh m^{-2}, or roughly 15 % of the 50–70 kWh m^{-2} baseline. Within that narrow band, however, a hierarchy emerged. Locating the fabric blind on the façade exterior consistently produced the most favourable energy balance, cutting heating in Stockholm and Frankfurt by around fifteen percent and halving it in Rome, while also trimming cooling demand in the cooler climates, compared with inernally locaded fabric blind. Electrochromic glazing occupied the middle ground—lowering heating relative to an interior blind but incurring more cooling than an exterior screen. Moreover, the variability of fabrics, in terms of color and opennes factor, proved to be the least effective in terms of energy performance.

Daylight performance followed a climate-dependent pattern: the exterior blind boosted spatial daylight autonomy in the diffuse northern climates yet reduced it in the bright Mediterranean context, where a light-coloured interior blind or electrochromic glass performed best. Glare analysis revealed only modest spread among fabric blinds but showed that electrochromic glazing edged DGP upward, enough to shift its EN 17037 rating from “imperceptible” to “perceptible” glare. In non-visual daylight potential analysis, mel-DA, as its indicator, exceeded 70 % for every option in Stockholm and Frankfurt, whereas in Rome it spanned 65–88 %, with electrochromic glazing and pearl fabrics at the upper end and dark interior blinds at the lower. Finally, parametric control testing demonstrated that the control algorithm design mattered as much as, and sometimes more than, the hardware itself; for example, switching from a crude irradiance trigger to a DGP-based rule altered annual energy use by up to a dozen kilowatt-hours per square metre.

5.2 Implications for design practice

For practitioners, the most actionable message is that moving a shade to the building exterior often delivers a larger efficiency and daylight boost than upgrading the glazing to a dynamic technology. Where exterior devices are impractical because of wind exposure, heritage constraints or maintenance concerns, electrochromic glazing offers a robust fallback, provided its slightly higher peak-glare risk is mitigated through furniture layout or supplementary interior baffling. Regardless of the hardware selected, the study highlights the need to commission the control system with the same care given to the glass or fabric specification: sensors should reference occupant-centred metrics such as DGP or work-plane illuminance rather than generic irradiance cut-offs, and the logic must recognise the fundamentally different heat-transfer behaviour of interior versus exterior mounts.

5.3 Research directions

Several simplifications in the present work point to fruitful avenues for future investigation. Testing the same façade set in an open-plan office would capture inter-desk reflections and deeper room geometries that may alter both daylight and energy outcomes. Incorporating hourly wind speed into the exterior-blind model would clarify how often safety lock-outs erode the predicted energy savings. Introducing Venetian oblinds would allow comparison of angular-selective systems with the woven fabrics and electrochromic glass evaluated here. View quality analysis also depends on developing a validated metric that combines colour shift, obstruction ratio and unsharpness so that view quality can be compared across technologies. Finally, coupling physics-based simulations with user assessment cosniderations would reveal whether the theoretically optimal control strategies align with real occupant preferences and override behaviour.

5.4 Concluding statement

Dynamic façades can readily meet demanding energy and daylight comfort targets across diverse climates, but their ultimate success hinges less on exotic materials than on thought-ful placement and adaptive, occupant-centred control. By directing future innovation toward robust algorithms, context-aware deployment and metrics, the building industry can provide more accurate dynamic facade towards human health and comfort.

Appendix A

Conference Paper - CISBAT

Comparing the performance of electrochromic glazing and fabric blinds under automated and manual control schemes in office buildings

M Sabeti[1,2], H Khodaei Tehrani[1], V R M Lo Verso[3], J Wienold[1]

[1]School of Architecture, Civil and Environmental Engineering, Laboratory of Integrated Performance in Design (LIPID), École polytechnique fédérale de Lausanne (EPFL), Lausanne, Switzerland
[2]Dept. of Architecture and Design, Politecnico di Torino, Turin, Italy
[3]Dept. of Energy 'Galileo Ferraris', TEBE Research Group, Politecnico di Torino, Turin, Italy

mojdeh.sabeti@studenti.polito.it

Abstract. This study compares the performance of electrochromic (EC) glazing and fabric roller blinds under automated control with manual override in office buildings across three European climates including Stockholm, Frankfurt, and Rome. A simulation-driven methodology using a single-office layout with dual occupancy assessed key performance metrics: energy demand, indoor daylight provision, daylight glare, and daylight-induced non-visual potential. Fabric blinds were evaluated in both internal and external configurations, paired with solar control or Low-E glazing. EC glazing was analysed with independently controlled upper and lower window sections. Realistic sensor-triggered control strategies with specified thresholds were applied. Results show overall differences between shading solutions are modest. However, external shading and EC enhance energy efficiency in cooler climates (Stockholm and Frankfurt), while in Rome, EC glazing performs similarly to internal shading. EC also exhibits a slight increase in glare for all investigated climates. Spatial daylight autonomy was the highest for external shading in cooler climates and lowest in Rome, and non-visual potential were high for all systems in Stockholm and Frankfurt, while it shows variations in Rome. This study also concludes that control strategy plays a more decisive role in optimizing façade performance than the shading technology itself, underscoring the importance of developing optimized control algorithms.

1. Introduction

In recent years, the integration of dynamic shading and facade technologies, such as EC glazing and fabric roller blinds, has emerged as an effective strategy for enhancing energy efficiency while addressing occupant comfort in offices [1]. These responsive systems can improve the building performance by integrating energy and daylighting control strategies and occupant behavior [2].

Fabric shading systems are commonly used worldwide as a solution for regulating solar gains and mitigating glare in office settings. Their performance can be enhanced through selection of materials and their properties, such as openness factor and color, and also through an optimized control scheme [3-5]. On the other hand, EC glazing offers a dynamic window solution that adjusts its tint to control the solar penetration into the building. This adaptive response not only reduces energy demand but also maintains a favorable balance between daylight penetration and visual comfort [6-7].

While both fabric blinds and EC glazing have been extensively studied in isolation, direct comparisons in office environments remain limited. A recent comparative investigation evaluated these technologies under multiple control algorithms. It underscores the importance of simulation method for

performance assessment, and also the necessity of considering effective control schemes [8]. Building on these insights, the present study aims to assess the performance of EC glazing and fabric blinds under automated control with manual override in office buildings in different climates. By examining their impacts on energy demand, indoor daylight provision, glare perception, and daylight-induced non-visual potential, this research seeks to provide a comprehensive framework that informs the selection and implementation of dynamic façade technologies for office design under varying climatic conditions.

2. Methodology

The methodology uses simulation-driven analysis on a two-occupants office layout (Figure 1) and is applied across three climates, Central (Frankfurt), Northern (Stockholm), and Southern Europe (Rome).

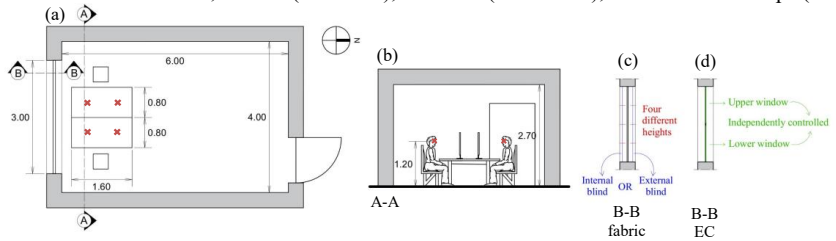

Figure 1. Office configuration and element; The red crosses represent the position of the sensors. (a) Plan. (b) Section A-A (c) Section B-B, Window with fabric roller blinds. (d) Section B-B, Electrochromic glazing.

2.1 Configuration and material properties

This study investigates fabric roller blinds installed either externally or internally. External blinds are paired with low-emissivity (Low-E) glazing, while internal blinds use solar control glass, chosen as adequate solutions for balancing daylight and energy performance [9-10]. Three fabric types, including black, pearl, and black-metallized (black fabric with one metallic-coated side), are analysed with 1% and/or 3% openness factors, using synthetic data based on typical real-world products. Glazing properties for both glass types and EC are sourced from the LBNL Window tool [11], and the EC configuration uses a commonly applied blue-tinting version [12] (Table 1).

Table 1. Material properties of fabrics and glazings.

	Black fabric		Pearl fabric		Metalized fabric	LowE glazing	Solar control glazing	EC			
								S_{e0}	S_{e1}	S_{e2}	S_{e3}
OF[a] [%]	1	3	1	3	3	-	-	-	-	-	-
τ_v^* [%]	1	3	9	9	3	78	59.4	56.6	34.3	5	1.2
τ_e^* [%]	1	3	9	9	4	53	26	30.5	15	2	0.5
SHGC[b][%]	-	-	-	-	-	60.4	30.5	37	21.2	8.1	6.6

[a] The openness factor (OF) cannot be applied to glazing.

[b] The Solar Heat Gain Coefficient (SHGC) of the fabric is determined in conjunction with the glazing configuration.

*τ_v: visual transmittance; τ_e: solar transmittance.

2.2 Control strategy – during usage hours

Usage hours include the working days from 8 a.m. to 6 p.m., excluding the weekends as holidays. For dynamic shading responses, six virtual sensor grids are defined to trigger control activation caused by glare (sun hits eye or desk): four horizontal sensors on the desk and two vertical sensors at eye level with perpendicular view direction (Figure 1). Fabric blind control is based on dynamic height adjustment to enable comparison with EC which offers multiple tint levels. For EC, the window is divided into one upper and one lower section, each with independently controlled glazing. The following sections describe the control schemes for each configuration.

2.2.1 Solar control glazing + internal fabric blinds (sc+ib): Glare-avoidance control only. This control scheme uses glare-avoidance rules only and predicts manual behaviour, where shading is triggered by

glare metrics and solar exposure, mimicking occupant actions. Solar gain control was ineffective for this system, because it showed either no measurable reduction in cooling load or a slight increase. Such marginal energy effects do not justify the accompanying compromise on daylight performance, particularly because the glazing itself already provides solar-control properties. The activation is based on occurrence of direct sun in the occupant's field of view (DS-FOV) or on the desk (DS-D).

An activation signal is triggered for the fabric blind when: (i) direct sun is visible for the occupants, and (ii) DGP exceeds 0.35. The blind is lowered to block sunlight and reduce DGP below 0.35. If DGP remains above 0.35 despite shading, the blind stays at the height where the minimum DGP is achieved.

A separate rule applies to desk sensors: shading is activated when direct sun reaches the desk and vertical façade Irradiance (I_v) exceeds 450 W/m^2 (this value is assumed by trial and errors to avoids overestimating the shading activation). This ensures to mitigate high-intensity sunlight causing reflection/high contrast on the desk (Figure 2).

2.2.2 Low-E glazing + external fabric blinds (lowE+eb): Glare-avoidance control and Solar-gain control. This control scheme combines glare control, which follows the same method as Section 2.2.1, with solar gain control. This control is based on: (1) vertical façade Irradiance (E_f), and (2) ambient air temperature. Shading is activated when: (i) $E_f \geq 150$ W/m² [13], and (ii) the 168-hour moving average temperature (T_{rm}) is over 17 °C (control is in "summer-mode"). In this case, the external blind is lowered to 3/4 height to reduce overheating while preserving view and daylight (Figure 2).

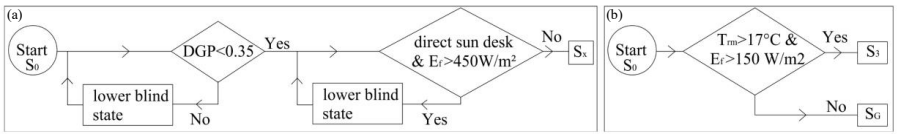

Figure 2. Fabric blind control scheme defining blind state S. (a) Glare avoidance control. S_x with x[0…3] based on glare. (b) Solar gain control. S_0: no shading, S_1: 1/4 of fabric height, S_2:2/4 of height, S_3:3/4 of height.

2.2.3 Electrochromic glazing – upper window: Glare-avoidance control and Solar-gain control. Glare-avoidance control is applied by tinting the EC window based on direct sun exposure detected by vertical sensors at eye level and horizontal desk sensors. As shown in Figure 3, when sunlight is detected, the window will be tinted accordingly, and solar gain control follows the same logic as for external fabric blinds, but with more defined thresholds for tint transitions, confirmed by manufacturers.

2.2.4 Electrochromic glazing – lower window: Solar-gain control only. No glare-avoidance control is applied to the lower EC glazing, as it lies below the 1.2 m eye level of seated occupants. However, a solar gain control strategy, similar to the upper window, is implemented to reduce overheating, with specific thresholds defined for each tint level (Figure 3).

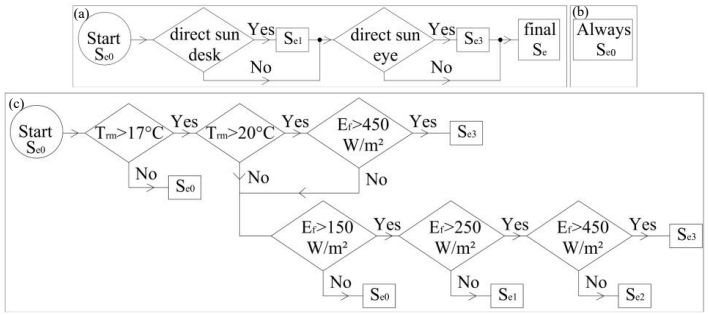

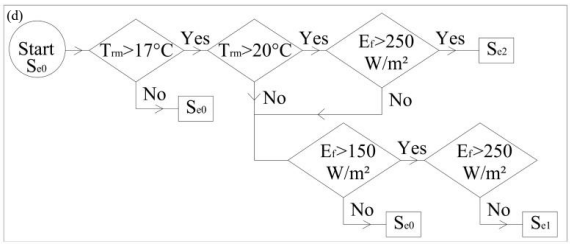

Figure 3. Electrochromic glazing control scheme defining glazing state S_e. Glare avoidance control: (a) upper window. (b) lower window. Solar gain control: (c) upper window. (d) lower window. $S_{e\,[0\ldots3]}$: refer to Table 1.

2.3 Control strategy – outside usage hours

An additional control strategy is applied during non-occupied hours, i.e. weekends and weekdays from 6 p.m. to 8 a.m., to optimize solar heat gains and losses based on seasonal conditions. In summer-mode, when the T_{rm} exceeds 17 °C: (1) fabric blinds are fully lowered, and (2) EC glazing is set to its darkest state. This avoids interior overheating and storing the gains in materials with higher inertia, leading to cooling loads reduction. In non-summer periods, the strategy enables passive heat gain: (1) fabric blinds remain retracted, and (2) EC glazing stays clear, supporting indoor heating needs.

2.4 Performance metrics and simulation tools

Analysed performance metrics are energy demand for heating, cooling, and interior lighting, indoor daylight provision, glare perception, and daylight-induced non-visual potential. The 3D model is developed in Rhino, and the engines in Grasshopper (Honeybee (HB) and Ladybug (LB) tools) [14] used as the general tool to: (1) assign construction and weather data [15] to the model, (2) simulate energy demands, and (3) evaluate spatial daylight autonomy (sDA) as the indicator to assess daylight provision. sDA is simulated using the BSDF files generated by genBSDF [16] and processed with a validated method [17] used in EN 14501 and EN17037.

95th percentile of the hourly Daylight Glare Probability is calculated using Raytraverse [18] due to its capability to accurately predict glare from sun seen through shades, unlike the module in HB and LB which is incapable for this purpose. For the calculation of the daylight-induced non-visual potential, with Melanopic Equivalent Daylight Illuminance (mel-EDI) as the main indicator, we assumed internal materials and the fabric to be colour-neutral preserving the relative spectral distribution of light, while all glazing types including EC and its tint variations change it. To evaluate mel-EDI, the Melanopic Daylight Efficacy Ratio (mel-DER) for all glazings is obtained via a validated Excel tool [19] (Table 2), and the photopic illuminance (E_p) via Raytraverse. As daylight entering the space is only altered through the glazing, the mel-EDI can be determined by modifying the photopic illuminance through the mel-DER: mel-EDI= E_p * mel-DER. The non-visual potential is evaluated as the percentage of daytime hours with mel-EDI > 250 lux [20] at eye level, defining the melanopic daylight autonomy (mel-DA).

Table 2. The melanopic daylight efficacy ratio (mel-DER) of different glazings. First row shows the glazings, and the second row represents the equivalent mel-DER for each glazing.

		EC			
Solar control glazing	LowE glazing	S_{e0}	S_{e1}	S_{e2}	S_{e3}
1.02	1.00	0.90	0.96	1.36	1.52

3. Results

Table 3 shows the frequency of the activation states for each shading system in each climate, depending on the sun angle, the duration of summer period, and other climatic aspects, as a result of the applied shading control algorithms. The occurrence of half and 3/4 of fabric height was relatively frequent for all the climates, and although they provide a better view compared with full height, they can reduce the clarity of the view. The EC darkest state is also frequently activated, which may also disturb view clarity.

Table 3. The frequency of activation states (during usage hours) for different shading system is each climate.

	Frankfurt			Stockholm			Rome		
State	sc+ib[a] [%]	lowE+eb[b] [%]	EC[c] [%]	sc+ib[a] [%]	lowE+eb[b] [%]	EC[c] [%]	sc+ib[a] [%]	lowE+eb[b] [%]	EC[c] [%]
0	23	34	36	35	30	34	36	15	42
1	12	19	25	13	8	26	19	13	20
2	36	31	2	34	41	4	22	28	2
3	29	16	37	18	21	36	23	42	36

[a] Solar control glazing + internal fabric blinds
[b] Low-E glazing + external fabric blinds
[c] For electrochromic (EC) glazing, only the activation frequency for the upper window is represented.

Figure 2a,b,c show comprehensively the results for all calculated metrics for the three different locations. The evaluation reveals, as expected, that the climatic conditions significantly influence the energy requirements for heating, cooling, and interior lighting. In the absence of mechanical ventilation with heat recovery, the elevated heating values observed across all climates are expected. Overall, the differences between the various configurations in terms of overall performance are small. In Frankfurt and Stockholm, the heating demand for the lowE+eb and EC is 15% lower compared to the sc+ib options. In Rome, however, the heating demand of lowE+eb is 45% lower than that of sc+ib, while the performance of EC is similar to sc+ib.

The analysis of the annual DGP (95th percentile value during usage time) reveals that the values remain relatively consistent across different fabric shading configurations within each climate, with a marginal increase noted for EC glazing. This increase shifts the glare perception classification according to EN17037 from “high” to “medium” [21]. Conversely, the sDA metric exhibits distinct behaviour across the climates: lowE+eb results in higher sDA in Frankfurt and Stockholm, whereas in Rome, sDA is lower for lowE+eb, always compared to the other shading solutions in the respective climate. This is likely due to prolonged summer conditions and the activation of solar gain control measures. Regarding the daylight non-visual potential, as indicated by the mel-DA, Stockholm and Frankfurt show similar results across all configurations on a high level (>70% of time with mel-EDI>250lux). In Rome, however, mel-DA values are higher using lowE+eb, sc+ib with a light fabric colour, and EC.

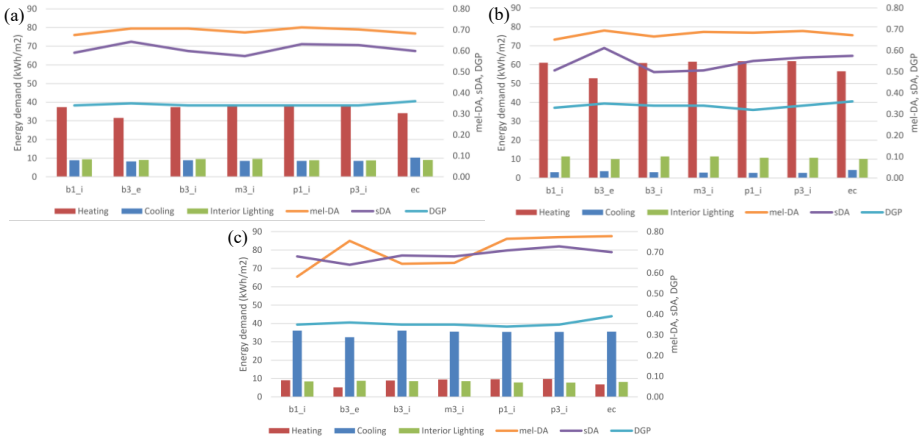

Figure 4. Final result for (a) Frankfurt, (b) Stockholm, (c) Rome. Configuration naming: b(black), p(pearl), m(metalized), ec(electrochromic) , 1(openness factor:1%) , 3(openness:3%), i(interior), e(exterior)

4. Discussion

The results in this study show that the overall differences between shading configurations are small, with external shading as a generally better solution for all the climates compared to EC and internal

shading. Moreover, EC showed a better energy performance than internal blinds, while in the comparative analysis by Alkhatib et al. [8], generally, EC was performing better than roller blinds which are "in-between" the window glazings. This shows the importance of the shading position in the final energy and daylight performance.

4.1 Importance of control strategies

Through the process of developing the control scheme, one of the key findings was that control strategy plays a more significant role in performance than the shading technologies, as it also demonstrated in the analysis by Alkhatib et al [8]. For instance, for the glare-avoidance control, initially a threshold of 120 W/m² for direct irradiance, based on World Meteorological Organization [22], was considered to define sunshine hours. However, this threshold resulted in high DGP values by sunlight passing through the glass, and even lower values (e.g., 40 W/m²) resulting in DGP values in the range of 0.6. Consequently, DGP values were directly implemented in the control strategy as it should reflect user interaction with the shades when glare is present.

4.2 Limitations and future development

Although this study provides valuable insights, it did not include also open-plan office layout. Moreover, while external shading proved to be efficient across climates, the effects of wind speed were not incorporated. High-speed winds may impede shading activation, potentially increasing cooling demand in Rome or resulting in an increased incidence of glare in Stockholm and Frankfurt. In addition, the study did not include Venetian blinds, which, due to their angular dependency and flexibility, might enhance external shading performance. Future work integrates wind speed data and also analysis of Venetian blinds.

Another limitation is Another limitation is the absence of an accurate assessment of the view quality, as colour shifts in EC glazing, partial view blockage and refraction in fabrics, make them incomparable due to the lack of validated metrics. Finally, the control strategies did not incorporate user assessments, which could provide more nuanced insights into occupant behaviour.

5. Conclusion

This study compares the performance of dynamic shading systems, EC and fabric roller blinds, under automated control with manual override in office environment, through analysis of energy demand, daylight provision, glare perception, and daylight-induced non-visual potential across different climates. The research demonstrates that the overall performance of the investigated shading options is similar, however, the energy performance of external shading and EC is better in cooler climates (Frankfurt and Stockholm), with EC becoming similar to internal shading in warm climate (Rome).

The study further identifies that EC tends to slightly intensify glare occurrence compared with external and internal shadings and sDA varies significantly depending on the shading configuration and climate. External shading results in higher sDA in Frankfurt and Stockholm, whereas in Rome, sDA is lower for external blinds, compared to the other shading solutions. Also, the daylight non-visual performance, follows similar trends across climates, but with higher values under certain shading conditions in warmer regions. The findings also show that the control strategy has a larger impact on the performance than the shading technologies. Consequently, future research should place greater emphasis on optimizing the integrated control schemes within shading technologies.

Acknowledgements

The author acknowledges Politecnico di Torino and extends special thanks to LIPID lab at EPFL for hosting the research activities.

Credit author statements

Mojdeh Sabeti: Methodology, Software, Validation, Formal analysis, Data Curation, Visualization, Writing–Original Draft, Writing–Review & Editing. **Hanieh Khodaei Tehrani:** Methodology, Validation, Software, Writing–Review & Editing. **Valerio R.M. Lo Verso:** Writing–Review & Editing, Supervision. **Jan Wienold:** Conceptualization, Methodology, Validation, Writing–Review & Editing, Supervision, Resources.

References

[1] Gonçalves M, Figueiredo A, Almeida RMSF and Vicente R 2024 Dynamic façades in buildings: A systematic review across thermal comfort, energy efficiency and daylight performance *Renewable and Sustainable Energy Reviews* **199** 114474

[2] Alkhatib H, Lemarchand P, Norton B and O'Sullivan DTJ 2021 Deployment and control of adaptive building facades for energy generation, thermal insulation, ventilation and daylighting: A Review *Applied Thermal Engineering* **185** 116331

[3] Karmann C, Chinazzo G, Schüler A, Manwani K, Wienold J and Andersen M 2023 User assessment of fabric shading devices with a low openness factor *Building and Environment* **228** 109707

[4] Bavaresco MV, Geraldi MS, Balvedi BF and Ghisi E 2019 Influence of control and finishing of internal blinds on the cooling energy consumption of buildings *Building Simulation Conference proceedings* (Rome: IPBSA Publications) **16** 2270–77

[5] Lu S, Wang T and Tzempelikos A 2024 Glare-based selection of roller shade properties *Building and Environment* **265** 111954

[6] Fathi S and Kavoosi A 2021 Effect of electrochromic windows on energy consumption of high-rise office buildings in different climate regions of Iran *Solar Energy* **223** 132–49

[7] Anissa Tabet Aoul K, Attoye DE and Al Ghatrif L 2019 Performance of electrochromic glazing: State of the art review *IOP Conf. Ser.: Mater. Sci. Eng* **603(2)** 022085

[8] Alkhatib H, Lemarchand P, Norton B and O'Sullivan DTJ 2023 Comparative simulations of an electrochromic glazing and a roller blind as controlled by seven different algorithms *Results in Engineering* **20** 101467

[9] Khalaf M, Ashrafian T and Demirci C 2019 Energy efficiency evaluation of different glazing and shading systems in a school building *E3S Web of Conference* (Bucharest: EDP Sciences) **111** 03052

[10] Singh R, Lazarus IJ and Kishore VVN 2015 Effect of internal woven roller shade and glazing on the energy and daylighting performances of an office building in the Cold Climate of shillong *Applied Energy* **159** 317–33

[11] Lawrence Berkeley National Laboratory 2022 WINDOW (version 7.8.55) Online: https://doi.org/10.11578/dc.20210416.62

[12] Kraft A 2024 Too blue to be good? A critical overview on the electrochromic properties and applications of Prussian blue *Solar Energy Materials and Solar Cells* **278** 113195

[13] Chinazzo G, Plourde M, Pereira J, Wienold J and Andersen M 2017 Sensitivity analysis of visual and thermal parameters for energy savings: Combining illuminance and temperature set-points for possible trade-offs *Building Simulation Conference Proceedings* (San Francisco: IBPSA Publications) **15** 1974-83

[14] Ladybug Tools LLC 2025 Ladybug Tools (version 1.8.111) Online: https://www.ladybug.tools/

[15] Crawley D and Lawrie L 2024 Repository of building simulation climate data From the creators of the EPW Online: https://climate.onebuilding.org/

[16] McNeil A, Jonsson CJ, Appelfeld D, Ward G and Lee ES 2013 A validation of a ray-tracing tool used to generate bi-directional scattering distribution functions for complex fenestration systems *Solar Energy* **98** 404–14

[17] Wang T, Lee ES, Ward GJ and Tammie Y 2023 Field validation of isotropic analytical models for simulating fabric shades *Building and Environment* **236** 110223

[18] Wasilewski S, Grobe LO, Wienold J and Andersen M 2022 Efficient simulation for visual comfort evaluations *Energy and Buildings* **267** 112141

[19] Houser KW, Esposito T, Royer MP and Christoffersen J 2022 A method and tool to determine the colorimetric and photobiological properties of light transmitted through glass and other optical materials *Building and Environment* **215** 108957

[20] Brown TM *et al.* 2022 Recommendations for daytime, evening, and nighttime indoor light exposure to best support physiology, sleep, and wakefulness in healthy adults *PLOS Biology* **20(3)** e3001571

[21] European Committee for Standardization 2018 Daylight in buildings. EN 17037:2018 (Brussels: CEN)

[22] World Meteorological Organization 2008 Guide to meteorological instruments and methods of observation Online: https://library.wmo.int/

Bibliography

[1] P. Gonçalves and *et al.*, "Dynamic façades for energy, thermal and daylight performance: A systematic review and bibliometric analysis," *Renewable and Sustainable Energy Reviews*, vol. INFILL, p. 114 474, 2024. DOI: 10.1016/j.rser.2024.114474.

[2] G. Jamilu and *et al.*, "Classification and techno-economic review of dynamic façade technologies," *Energy Reports*, vol. INFILL, INFILL, 2024. DOI: 10.1016/j.egyr.2024.05.047.

[3] X. Wang and *et al.*, "Dynamic façades: Typologies, physical performance and control strategies—a systematic review," *Journal of Building Engineering*, vol. INFILL, p. 111 310, 2024. DOI: 10.1016/j.jobe.2024.111310.

[4] H. Alkhatib and *et al.*, "Adaptive building façades: Multifunctional skins for high-performance envelopes," *Applied Thermal Engineering*, vol. INFILL, p. 116 331, 2021. DOI: 10.1016/j.applthermaleng.2020.116331.

[5] C. Karmann and *et al.*, "Glare–view trade-offs of roller-shade fabrics: A semi-controlled office experiment," *Building and Environment*, vol. INFILL, p. 109 707, 2023. DOI: 10.1016/j.buildenv.2022.109707.

[6] G. Bavaresco and *et al.*, "Influence of blind control logic and surface finish on office cooling loads," in *Proc. of Building Simulation 2019 (IBPSA)*, 2019, p. 210 794. DOI: 10.26868/25222708.2019.210794.

[7] Y. Lu and *et al.*, "Image-based annual glare assessment for roller shades using measured bsdfs," *Building and Environment*, vol. INFILL, p. 111 954, 2024. DOI: 10.1016/j.buildenv.2024.111954.

[8] A. Fathi and A. Kavoosi, "Whole-building impact of electrochromic glazing across four iranian climates," *Solar Energy*, vol. INFILL, p. 05.021, 2021. DOI: 10.1016/j.solener.2021.05.021.

[9] B. Al-Fasi and I. Budaiwi, "Daylight- and glare-triggered control of ec glazing in hot-humid offices," *Sustainability*, vol. 15, no. 12, p. 9632, 2023. DOI: 10.3390/su15129632.

[10] K. Tabet Aoul and *et al.*, "Electrochromic glazing: Performance, design and market challenges," in *IOP Conference Series: Materials Science and Engineering*, vol. 603, 2021, p. 022 085. DOI: 10.1088/1757-899X/603/2/022085.

[11] H. Alkhatib and *et al.*, "Comparing electrochromic glazing and roller blinds under advanced control algorithms," *Results in Engineering*, vol. INFILL, p. 101 467, 2023. DOI: 10.1016/j.rineng.2023.101467.

[12] J. Khalaf, A. Tavasolli, and Ö. Kaya, "Performance ranking of glazing–shading combinations for primary-school façades in istanbul," in *E3S Web of Conferences*, vol. 111, 2019, p. 03 052. DOI: 10.1051/e3sconf/201911103052.

[13] B. Singh, S. Mahapatra, and S. Singh, "Daylighting and energy analysis of high-performance glazing with permeable roller shades in cool, overcast climates," *Applied Energy*, vol. 159, pp. 807–822, 2015. DOI: 10.1016/j.apenergy.2015.09.009.

[14] A. Tzempelikos and A. K. Athienitis, "The impact of shading control on building energy consumption," *Solar Energy*, vol. 81, no. 3, pp. 369–382, 2007. DOI: 10.1016/j.solener.2006.06.015.

[15] M. Rosencrantz, "Solar control of office windows: Laboratory measurements and parasol simulations," Ph.D. dissertation, Lund University, Lund, Sweden, 2005, ISBN: 91-85147-13-3.

[16] T. E. Kuhn, "Calorimetric determination of solar heat-gain coefficients of glazing–shade systems," *Energy and Buildings*, vol. 84, pp. 388–401, 2014. DOI: 10.1016/j.enbuild.2014.08.021.

[17] M. Kraft, "Too blue to be good? a critical review of prussian-blue electrochromics for large-area smart windows," *Solar Energy Materials and Solar Cells*, vol. 259, p. 113 195, 2024. DOI: 10.1016/j.solmat.2024.113195.

[18] G. A. Niklasson and C. G. Granqvist, "Electrochromics for smart windows: Thin-film oxide materials and devices," *Journal of Materials Chemistry*, vol. 17, no. 2, pp. 127–156, 2007. DOI: 10.1039/B612174H.

[19] Y. Wu and *et al.*, "Electrochromic smart windows: Materials, devices and building-scale performance," *Cell Reports Physical Science*, vol. 4, no. 12, p. 101 370, 2023. DOI: 10.1016/j.xcrp.2023.101370.

[20] R. McNeel and Associates. "Rhinoceros [computer software]," Accessed: Aug. 1, 2025. [Online]. Available: https://www.rhino3d.com/.

[21] R. McNeel and Associates. "Grasshopper [computer software plug-in]," Accessed: Aug. 1, 2025. [Online]. Available: https://www.grasshopper3d.com/.

[22] "Ladybug tools, Making environmental design knowledge and tools freely accessible to every person, project and design process." Accessed 28 July 2025, Ladybug Tools, Accessed: Jul. 28, 2025. [Online]. Available: https://www.ladybug.tools/.

[23] Lawrence Berkeley National Laboratory. "WINDOW: A tool for simulating window thermal and optical performance." Accessed 23 July 2025, Accessed: Jul. 23, 2025. [Online]. Available: https://windows.lbl.gov/software/window.

[24] European Committee for Standardization, *EN 17037:2018 (E) — Daylight in buildings*, See Clause 5.4 and Annex E (glare) for the DGP definition and requirements, Brussels: CEN, 2018.

[25] G. Chinazzo, M. Plourde, J. Pereira, J. Wienold, and M. Andersen, "Sensitivity analysis of visual and thermal parameters for energy savings: Combining illuminance and temperature set-points for possible trade-offs," in *Proceedings of Building Simulation 2017 (IBPSA)*, 2017, p. 530. DOI: 10.26868/25222708.2017.530.

[26] L. K. Lawrie and D. B. Crawley. "Climate.onebuilding.org, Free climate data for building-performance simulation." Accessed 28 July 2025, Accessed: Jul. 28, 2025. [Online]. Available: https://climate.onebuilding.org/.

[27] A. McNeil, J. C. Jonsson, D. Appelfeld, G. J. Ward, and E. S. Lee, "A validation of a ray-tracing tool used to generate bi-directional scattering distribution functions for complex fenestration systems," *Solar Energy*, vol. 98, pp. 404–414, 2013. DOI: 10.1016/j.solener.2013.09.032.

[28] G. J. Ward et al., "Modeling specular transmission of complex fenestration systems with data-driven BSDFs," *Building and Environment*, vol. 196, p. 107 774, 2021. DOI: 10.1016/j.buildenv.2021.107774.

[29] *Light and lighting — basic terms and criteria*, Clause 3.1.8, CIE ILV term 17-492, Brussels, 2018.

[30] J. Wienold and J. Christoffersen, "Evaluation methods and development of a new glare prediction model for daylight environments with the use of ccd cameras," *Energy and Buildings*, vol. 38, no. 7, pp. 743–757, 2006. DOI: 10.1016/j.enbuild.2006.03.017. [Online]. Available: https://doi.org/10.1016/j.enbuild.2006.03.017.

[31] J. Wienold, "Dynamic daylight glare evaluation," in *Proceedings of Building Simulation 2009 – 11th International IBPSA Conference*, Glasgow, United Kingdom: International Building Performance Simulation Association (IBPSA), 2009, pp. 944–951.

[32] S. Wasilewski, L. O. Grobe, J. Wienold, and M. Andersen, "Efficient simulation for visual comfort evaluations," *Energy and Buildings*, vol. 267, p. 112 141, 2022, ISSN: 0378-7788. DOI: 10.1016/j.enbuild.2022.112141.

[33] *CIE System for Metrology of Optical Radiation for ipRGC-Influenced Responses to Light*, Standard, Vienna, Austria, 2018. DOI: 10.25039/S026.2018. [Online]. Available: https://doi.org/10.25039/S026.2018.

[34] K. W. Houser, T. Esposito, M. P. Royer, and J. Christoffersen, "A method and tool to determine the colorimetric and photobiological properties of light transmitted through glass and other optical materials," *Building and Environment*, vol. 215, p. 108 957, 2022. DOI: 10.1016/j.buildenv.2022.108957.

[35] Lawrence Berkeley National Laboratory, *Optics software for optical properties of glazing materials*, Version 6.0 and later. Available at: https://windows.lbl.gov/optics-downloads, Building Technologies Department, LBNL, 2020.

[36] T. M. Brown et al., "Recommendations for daytime, evening, and nighttime indoor light exposure to best support physiology, sleep, and wakefulness in healthy adults," *PLOS Biology*, vol. 20, no. 3, e3001571, 2022. DOI: 10.1371/journal.pbio.3001571.

[37] World Meteorological Organization. "Guide to meteorological instruments and methods of observation." Accessed: 2025-08-04, World Meteorological Organization. [Online]. Available: https://library.wmo.int/.